

1 Dear Dr. Lei Cai et al.,

2 Thank you for your responses to the Author's Comments. I recommend that you submit a
3 revised manuscript according to address the referee's comments and few more that I have
4 made that stem from their comments.

5 Re: Referee #2

6 Referee #2 seems generally satisfied with the revised version of the manuscript, but offers
7 a few major points and several minor points that you have indicated will be addressed in
8 your next revision. Your replies seem to address the questions adequately, with the exception
9 of the reply to R2's comment about your assumption on Line 220:

10 "Line 220: "Have the same area fraction of low ice landunit", You may add "(20%)" to make
11 it clearer. What is the reason behind this assumption?"

12 Please make the reason behind this assumption clear in the revised version of the manuscript.
13 I do not fully understand the logic as written in your Author's Reply.

14 Authors' reply: We have elaborated on the assumption in the revised manuscript.

15 Re: Referee #1

16 Referee #1 was not that satisfied with the revised version of the manuscript, and did not
17 provide comments on the Results and Discussion as a consequence. R1's major criticisms
18 still stem from initial concerns raised in the first round of reviews that there was (i) not enough
19 demonstration of the empirical basis for the parameterization of excess ice, and (ii) that
20 knowledge and understanding gained from empirical ground ice studies needs to be made
21 clearer to the reader. R1 provided several detailed points to help crystalize the issues.

22 Having read through your Author's Reply to R1, I have the following suggestions for you
23 to incorporate into your next revision:

24 As you say you intend to, please ensure that you state early on a clear scope and what the
25 great limitations are.

26 Authors' reply: We have clarified the scope and limitations of this study (model development)
27 in both the introduction and discussion sections in the revised manuscript.

28 Regarding terminology around ground ice content, I hope that it is made clear in the revised
29 version. In the Author's Reply you say "we emphasize that volumetric ice content in this
30 study refers only to excess ice bodies", but this is not how most readers think of volumetric
31 ice content. Volumetric ice content is pore ice + excess ice. If you use the term "volumetric
32 excess ice", it must always mean the volume ice in excess of the pore ice. The terminology
33 must be reconciled, made clear to the reader, and agree with how the terms are commonly
34 defined.

35 Authors' reply: We have now refined the terminology throughout the manuscript. Now we
36 have changed the "volumetric ice content" to "volumetric content of excess ice" or
37 "volumetric excess ice content" in order to emphasize that the ice content we refer to is
38 only for the excess ice bodies that exceed the soil pore space. For the volumetric content of
39 ground ice that includes both excess ice and pore ice, we keep using the term "volumetric
40 content of total ground ice" or "total volumetric ice content" for clarification. One exception
41 is that the ice content of the CAPS data, for which we keep using "volumetric ice content"
42 to keep the terminology consistent with the source data. As suggested by the R1, in the

43 revised manuscript we clarify that the “volumetric ice content” is approximately equal to
44 the “volumetric content of excess ice” in our study because the production of CAPS data is
45 mostly based on the visible excess ice bodies (Heginbottom et al. 1995).

46 Regarding excess ice content outside of the Yedoma Region, I suggest that you try to follow
47 R1’s comment and develop a way to better initialize wedge ice types that are not within
48 Yedoma deposits. R1 makes a good suggestion to “overlay CAPS and Yedoma areas in a
49 GIS and examine the overlap within chf, chr, and dhf to better inform and substantiate
50 landunit parameterizations/area weights”, which should be follow up on in the revised
51 manuscript. Perhaps also have a look at O’Neill et al. (The Cryosphere, 13, 753–773, 2019,
52 <https://doi.org/10.5194/tc-13-753-2019>).

53 Authors’ reply: We agree that the reviewer has given constructive suggestions on the
54 initialization of high ice landunit, while we did not follow his advice for several reasons. One
55 reason we have mentioned in the reply to R1 that this new scenario on high ice landunit does
56 not decrease the uncertainty of excess ice initialization on the global scale. There is also a
57 technical issue for the current version of our model development that it does not support
58 freely configuring excess ice volumetric contents for landunits in different grid points, which
59 means that all the high ice landunits in the same domain have to have the same excess ice
60 cryostratigraphy. Making it possible to initialize different cryostratigraphies for the same
61 excess ice landunit but in different locations needs substantial changes in the source code and
62 surface data variables, which probably should be regarded as a new version. Since all model
63 development work needs several updates since the release of the first version, we have
64 planned to add the function of freely configuring excess ice stratigraphy for each grid
65 point/landunit in the upcoming version, which is also dependent on the new excess ice
66 datasets. We have added text in the discussion section about the limitations and potential
67 improvements of our current model development on excess ice initialization scenario and
68 excess ice landunits assignments.

69 In your response to R1’s comment 3, you state a caveat about the availability of ground ice
70 information helpful to your sub-grid representation:

71 “As we mentioned, there is a lack of dataset on ground excess ice with enough information
72 helpful for our sub-grid excess ice representation. For this reason, this is our best effort to
73 make a possible scenario of excess ice distribution based on the best dataset (the CAPS data)
74 at this time, even though it only provides generalized information and has been released for
75 more than 20 years. Due to the lack of adequate information in excess ice distributions, the
76 purpose of this study is not to make an accurate estimate of excess ice melt and surface
77 subsidence in the 21st century, but rather to develop a functionable process within a land
78 surface model on a global scale. Once there is a new generation of excess ice dataset, the CLM
79 with sub-grid excess ice representation is able to be operational and give more accurate
80 projections of excess ice melt and surface subsidences.”

81 Please make sure that you state something to this effect in the introduction. Stating the clear
82 purpose will set up clear expectations from the reader. This caveat should also be echoed in
83 the Discussion. Given all of the uncertainty, and the goal of making a functioning process
84 within the land surface model, it would be instructive to include a sensitivity analysis of the
85 effects of differing sub-grid excess ice representation.

86 Authors’ reply: We have added stuff about the scope and limitations of this model
87 development study in both the introduction and discussion. We keep our idealized simulation

88 and analysis of the sensitivity of different sub-grid distribution of excess ice (North Slope of
89 Alaska and Yakutsk) in the previous version of manuscript (tc-2019-230) and put it into the
90 supplemental material.

91 Regarding R1's point 4, I don't follow the calculation in your example. If the original soil
92 layer is 7.5 m thick (between 1 and 8.5 m), and you increase it's volume by 70%, 7.5×1.70
93 is 12.75. adding back the first 1 m of ground gives 13.75 m of hydrologically active soil, no?
94 Not sure how one arrives at 18.5 m of hydrologically active soil. In any case, please make
95 sure that the added content in the main text makes the model design clearer.

96 Authors' reply: In the example taken in the reply to R1, since the soil layer after adding excess
97 ice has the volumetric content of excess ice of 70%, the original soil layer takes 30% of the
98 volume. In this way, the new thickness of soil is calculated as $1 + 7.5 \times 0.7 \div 0.3 = 18.5$ (m).

99 Regarding R1's point 5, it perhaps stems from the initial set up of the reader's expectations.
100 You have indicated that you have added clarification in the new text to address this point. I
101 additionally suggest that if the purpose of the manuscript is "not to retrieve realistic excess
102 ice melt, but rather to compare the model results from this study and from Westermann et al.
103 (2016)", then this purpose needs to be stated explicitly, and the inclusion of comparisons to
104 empirical studies should be carefully done so as not to give the wrong impression.

105 Authors' reply: We have added clarification in this section that the single-point experiments
106 over the Lena River Delta are just for model evaluation so that we want to initialize excess
107 ice exactly the same as in Westermann et al. (2016) in order to compare the model results in
108 the two studies.

109 Regarding R1's point 6, I agree that the schematic should show how the model actually
110 represents ground ice in the grid point. Show the "squeezing". If the added ice is "evenly
111 distributed within each soil layer", please show this distribution. It is expected that this
112 representation is an abstraction, and not reality.

113 Authors' reply: After some discussion, we decided to remove the upper left panel of figure 3
114 to avoid misunderstandings. We think that the upper right part of figure 3 has already presented
115 the concept of "squeezing". We have also added text in the methodology section about
116 "squeezing" to make our statement clear.

117 Please note the references kindly provided by R1 and incorporate where appropriate.

118 Authors' reply: We have incorporated the references provided by R1.

119 I look forward to receiving your revised manuscript in the near future.

120 Best regards,

121 Peter

122

123 Anonymous Referee #1 Received and published: 1 June 2020 This is a resubmission of a
124 previous discussion paper that was retracted by the authors following review: [https://www.the-](https://www.the-cryosphere-discuss.net/tc-2019-230/)
125 [cryosphere-discuss.net/tc-2019-230/](https://www.the-cryosphere-discuss.net/tc-2019-230/). For context, my previous review is available here:
126 <https://doi.org/10.5194/tc-2019-230-RC1>.

127
128 The single-point modelling has been changed to simulate 3 geomorphic units in the Lena River
129 delta, rather than Yakutsk and the North Slope of Alaska in the initial submission. The global
130 simulations include comparison of a no ice case, sub-grid representation case, and a grid-
131 average case.

132
133 My main criticisms of the first submission were that (a) the results were not validated in any
134 meaningful way, (b) the empirical basis for the parameterization of excess ice was lacking, and
135 (c) that there was not a clear comprehension of empirical ground ice studies and knowledge of
136 ground ice conditions.

137
138 I have read up to the results section and made several observations pertaining to points (b) and
139 (c) above. The points below do little to reassure me of my concerns with (b) and (c) from the
140 previous version. Furthermore, in my previous review I pointed out that references mentioned
141 in text were missing from the reference list. I expected such a simple item would be remedied,
142 but in the first paragraph of the introduction alone, the following references are missing from
143 the list: Walter et al. (2006); Schaefer et al. (2011).

144
145 Given these concerns, I have not formally reviewed the results or discussion.
146

147 Authors' reply: We appreciate your valuable comments which have contributed much to this
148 new revision of our manuscript. Here we respond to your two (remaining) main concerns. The
149 individual points have been addressed below.

150
151 First of all, we have tried to clarify the scope of the study in the new manuscript, which is to
152 provide a proof-of-concept for how heterogeneous excess ground ice can be represented in a
153 global Land Surface Model (LSM) used in Earth System Models (ESMs). While much work
154 remains before excess ice is represented in a fully satisfactory way in ESMs, we believe this
155 study represents an important step forward compared to the current generation models, which
156 for the most part fully ignores excess ground ice (only representing pore ice). Much
157 development of CLM (and other LSMs) in recent years have aimed at mechanistic
158 representation of key features, even when improvements to the model performance cannot be
159 demonstrated. As an example, the latest version of CLM showed an apparent degradation in
160 representation of snow water equivalent at global scale, despite mechanistic improvements in
161 snow physics (Lawrence et al. 2019). We believe our model enhancement is in line with this
162 aim, as it accounts for the effect of heterogeneous excess ice on hydrology and thermal
163 properties in a physically sound way, even though there are great limitations in the current
164 study, especially related to the initialization of excess ice.

165
166 Secondly, we have now clarified the terminology. As you correctly pointed out, the previous
167 version of the manuscript was ambiguous here, which understandably gave concern about the
168 use of observational studies. We want to highlight here again that we fully recognize the
169 limitations in excess ice initiation in our study. The observational studies listed in the
170 manuscript are not intended to be replicated here but are used to motivate the use of three broad
171 excess ice classes, which should be revisited in future studies.

172
173
174
175
176
177
178
179
180
181
182
183
184
185
186
187
188
189
190
191
192
193
194
195
196
197
198
199
200
201
202
203
204
205
206
207
208
209
210
211
212
213
214
215
216
217
218
219
220
221

1. It is unclear from the text whether the authors appreciate the difference between “excess ice content”, “volumetric ice content”, and “visible ice content”, as the terms are seemingly used interchangeably or confused.

In different places in the paper, the authors have indicated the CAPS values represent volumetric ice content, excess ice content, and visible ice content. The authors have misinterpreted the legend for the Circum-Arctic Map of Permafrost (CAPS) in their Figure 2. They have altered the legend from the original map by removing the clause stating “visible ice in the upper. . .”, and now only indicate “Ground Ice Content: percent by volume”. They report ice contents from the Circum-Arctic Map as volumetric ice content (lines 216, 224) in the text. Then, in the figure 2 caption, they suggest the CAPS values represent the “Spatial distribution of excess ground ice” – very confusing. The CAPS legend, and the Permafrost Map of Canada (Heginbottom et al. 1995) legend on which the CAPS compilation is based, both clearly indicate that the ice content reported is the visible ice content (as the authors correctly indicate on line 177). The legend on the Heginbottom et al. (1995) map indicates this visible ice percentage accounts for “segregated ice, intrusive ice, reticulate ice veins. . .”. The percentages on the maps do not correspond to volumetric ice content (in the strict sense), which also include the pore ice fraction.

Lines 185 to 190, the authors report that Yedoma is “characterized by massive ice wedges leading to typical average volumetric ice contents in the range from 60% to 90%” (line 188). They then state: “We therefore set the volumetric excess ice content to 70%”. Nowhere in the text do the authors mention the soil porosity, which is key to estimating excess ice content given only volumetric ice content. For example, if one assumes a soil porosity of 0.5, then volumetric ice contents of 60-90% represent excess ice contents of about 10-40%. Assuming an excess ice content of 70% based on volumetric ice contents of 60-90%, as presented above, is problematic. I refer the authors to Harris et al. (1988) for definitions of volumetric ice content and excess ice content.

Other examples that seemingly use the terms interchangeably: Line 137-138 “volumetric ice contents ranging from 60-80%” and in the next sentence, “higher excess ice contents are found in Pleistocene sediments. . .”; Line 193 “For the low ice landunit, we assume both a significantly lower volumetric ice content and a smaller vertical extent of the excess ice body”; Table 1. The caption reads “excess ice initialization scenario”, but the table header indicates “Volumetric Ice content”. Presumably, porosity is available, so why not also present the readers with excess ice content?

Finally, the term “ice content” (line 198) is also used on its own, as is “Overall Ground ice content” in Table 2, further complicating interpretation by the reader. What type of ice content? I’m left wondering throughout.

Authors’ reply: We agree with the referee’s comments that the terminology about ice content is somewhat unclear throughout the manuscript that could lead to misunderstanding of the main purpose of this study. But we do not believe we misrepresented the physical properties of ground ice overall when incorporating them into the structure of the large scale land surface model. The physical properties of ground ice used in our model development is only for the excess ice bodies that exceed the pore space of soil. In our model development, we do not address pore ice physics because it is already represented in the original CLM model, with the output variable named “soilice”. The melting of “soilice” in the CLM5 does not cause surface

222 subsidence as this ice only exists as part of pore space. Therefore, we emphasize that volumetric
223 ice content in this study refers only to excess ice bodies. We agree that directly applying the
224 ground ice content in the CAPS data is not necessarily an accurate way, while we have to make
225 sufficiently simple classes of ice content levels to avoid over-parameterization. We think that
226 using the volumetric ice content provided by the CAPS data is generally valid for the purpose
227 of this research since the CAPS data is based mostly on “visible” ice bodies (Heginbottom et
228 al. 1995). We have clarified the definition of “volumetric excess ice content” following Harris
229 et al. (1989) in the methodology section. We have also discussed the limitation of applying the
230 ice content values in the CAPS data in our model development in the discussion section.

231
232 2. The authors suggest that high ice classes mapped on the Circum-Arctic Map of Permafrost
233 and Ground ice Conditions (CAPS), designated in the submitted paper text as chf, chr, and dhf
234 partly coincide with Yedoma areas and are “broadly oriented at the excess ice contents and
235 distribution in intact Yedoma” (line 186-87).

236
237 The high ice landunit is considered representative of Yedoma. I’d like to point out the two
238 maps below. Figure 1 shows the areas of chf, chr, dhf highlighted in red. Figure 2 C3 shows
239 the distribution of Yedoma from Schuur et al (2015). The area mapped as chf, chr, and dhf is
240 much more extensive than areas mapped as Yedoma. For example, a large portion of the
241 Canadian Arctic Archipelago (CAA) is mapped as chr: continuous permafrost that has high
242 visible ice content (>10%) and thin overburden cover (5-10m) and exposed bedrock. Most of
243 the CAA was glaciated and includes no Yedoma. It therefore seems inappropriate to me that
244 vast areas such as this include a considerable fraction of the high ice landunit in the modelling
245 that represents Yedoma. The high ice landunit cryostratigraphy (70% excess ice in the upper
246 ~8 m), may reasonably represent ice-rich Pleistocene deposits where permafrost has aggraded
247 syngenetically, or local areas where large bodies of buried glacial ice occur just below the
248 permafrost table. However, I can’t think of situations where 70% excess ice content in the
249 upper 8-10m would be reasonable for other deposits in which permafrost has formed
250 epigenetically, given the typical decline in ice content with depth in epigenetic permafrost (e.g.,
251 French and Shur, 2010; Fig.2; Gilbert et al, 2019). I realize the authors acknowledge that the
252 cryostratigraphies prescribed in the simulations are a coarse first-order approximation.
253 However, the assumption that areas mapped with high ice content on the CAPS include
254 significant areas where ground ice content is similar to thick Yedoma deposits, including those
255 defined on the CAPS map as chr, seems particularly unrealistic and poorly justified.

256
257 It would have been simple to overlay CAPS and Yedoma areas in a GIS and examine the
258 overlap within chf, chr, and dhf to better inform and substantiate landunit
259 parameterizations/area weights.

260
261 Authors’ reply: We agree that overlaying the Yedoma coverage information and the CAPS data
262 can give a better interpretation over the Yedoma region. However, the excess ice content and
263 located depth of ice wedges out of the Yedoma region is still unclear and lacks observational
264 support. Although we fully acknowledge the importance of accurately representing different
265 Yedoma cover in the model, for the sake of model representation of permafrost thaw processes,
266 having an accurate projection over the Yedoma region does not improve the projections of the
267 excess ice melt over the whole circum-arctic in general. Since the main purpose of our study is
268 to represent permafrost thaw processes on a global scale, we make a decision to initialize
269 different kinds of ice wedged ice as “Yedome type ice”. As we understand this may not be fully
270 representing reality, we added discussion on how these initialization scenarios brings
271 uncertainties to surface subsidence projections in the discussion section. The high excess ice

272 content and the relatively cold climate where the high ice landunit is located make the wedged
273 ice almost impossible to melt out completely by the end of the 21st century. The remaining part
274 of the excess ice at the bottom has little effect on the surface subsidence. In this way, surface
275 subsidence projections by 2100, initializing Yedoma type ice at the Yedoma region does not
276 substantially affect the final result in our model simulations.

277

278 As we write in the discussion section, the purpose of simulation on top of this first-order
279 scenario is to show how our model development can represent permafrost thaw processes on a
280 global scale. Our modeling result shows that the current version of the CLM5 can represent
281 permafrost degradation process with a wide range all the way from continuous to discontinuous
282 permafrost and even no permafrost with the developed sub-grid representation of excess ice.
283 The surface subsidence in the sub-grid representation produces greater heterogeneity to the
284 land surface. Talik forming can also be retrieved during the degradation process. All of the
285 above are novel progresses that no other state-of-the-art global land models can represent.

286

287 3. The authors provide a rationale for the excess ice content in the high ice landunit (for global
288 simulations), which is commented on above, but provide little rationale for the medium and
289 low ice content landunits (lines 193-200). One reference to an empirical study is provided (Line
290 197). The authors indicate that the excess ice content and distribution for the low ice landunit
291 “account for a wide range of different excess ice conditions found throughout the permafrost
292 domain” (line 197-198). It would have benefitted the reader if some of these excess ice
293 conditions were elucidated, with pertinent references.

294 Authors’ reply: The scenario we designed for the low ice landunit is based on previous studies
295 that the segregated ice is widely distributed throughout the permafrost area. We have added
296 more reference that segregated ice has been widely distributed throughout the permafrost area,
297 both continuous and discontinuous permafrost (Line 239-246). We also provide an additional
298 empirical excess ice volumetric content (25%) and located depth (ALT+0.2 ~ALT+1.2) to the
299 low ice landunit. For the mid ice landunit, the volumetric content of excess ice and located
300 depths are set in between the low and high ice landunits, which are also based on empirical
301 data. As we mentioned, there is a lack of dataset on ground excess ice with enough information
302 helpful for our sub-grid excess ice representation. For this reason, this is our best effort to make
303 a possible scenario of excess ice distribution based on the best dataset (the CAPS data) at this
304 time, even though it only provides generalized information and has been released for more than
305 20 years. Due to the lack of adequate information in excess ice distributions, the purpose of
306 this study is not to make an accurate estimate of excess ice melt and surface subsidence in the
307 21st century, but rather to develop a functionable process within a land surface model on a
308 global scale. Once there is a new generation of excess ice dataset, the CLM with sub-grid excess
309 ice representation is able to be operational and give more accurate projections of excess ice
310 melt and surface subsidences.

311

312 4. The authors state that subsidence of “more than 10 meters” (line 203) could occur if all ice
313 melted from the high ice landunit in the global simulations. Earlier, the authors indicate that
314 “we put excess ice in all the soil layers between 0.2 meters below the active layer and the
315 bottom of hydrologically-active soil layer (8.5 meters)”. As it is written, >10 m of subsidence
316 is implied from thaw of <8.5m of ground.

317

318 Authors’ reply: We have mentioned in the methodology section (Line 115) that the soil layer
319 depth increases accordingly after adding excess ice. In this way, the soil thickness with excess
320 ice added is thicker than 8.5 meters. For example, adding high ice landunit (70% volumetric
321 excess ice content) in the soil layers with the original depths between 1 and 8.5 meters can

322 make the thickness of hydrologically-active soil 18.5 meters in total. > 10 m of subsidence is
323 therefore possible in the simulation. We have added the content above in the main text to make
324 the model design clearer.

325

326 5. The authors indicate that abundant field data in the Lena River delta provide a good basis
327 for initializing ice conditions in refocused single-point simulations. I fully agree that
328 simulations in areas with good available data is crucial. However, the authors in fact report no
329 measurements of excess ice content anywhere in section 2.2 (only some volumetric ice contents
330 are provided). It would benefit the reader to have some of these examples if there is abundant
331 field data.

332

333 I am also confused by the authors' interpretation of the data that is presented in this section.
334 For example, in Line 136 the authors indicate that ice wedges extend to 9 m depth in the
335 Holocene terrain unit, and that there are volumetric ice contents of 60- 80%, citing
336 Schwarmborn et al. (2002) and Langer et al. (2013). Schwarmborn et al. (2002) indicate much
337 smaller ice wedges in the Holocene sediments: "and subaerial or buried ice wedges of 2–3m in
338 height and width are common." (p. 123), and I cannot find wedge dimensions in Langer et al.
339 (2013). I can only find mention of ice wedges that extend deeper (5-10 m) in the Ice Complex
340 (Yedoma) unit in Schwarmborn et al. (2002).

341

342 The volumetric ice contents of 60-80% reported for the Holocene unit are seemingly from
343 Langer et al. (2013, p.13) who indicate: "The elevated rims are usually covered with a dry moss
344 layer underlain by wet sandy peat soils featuring massive ice wedges. The volumetric water/ice
345 content of the peat soils typically ranges from 60 to 80%.". This value appears to refer to the
346 volumetric ice content of the mineral soil C5 between ice wedges, rather than to an average
347 representative value for a terrain unit or cross-section that includes both the icy soil matrix and
348 ice wedges. At the scale of the modelling, this is what is pertinent, otherwise the contribution
349 to ice content in the upper permafrost from ice wedges is not accounted for.

350

351 Authors' reply: For this single-point case for model evaluation, our goal is not to retrieve
352 realistic excess ice melt, but rather to compare the model results from this study and from
353 Westermann et al. (2016). Initializing realistic excess ice condition does not help the model
354 evaluation in this case because the Lena River Delta has observed hardly any surface
355 subsidence yet, making model-observation comparisons inapplicable. Alternatively, we make
356 model-to-model intercomparisons to evaluate our developed physics and sub-grid
357 representation. So we initialize excess ice strictly following that in Westermann et al. (2016).
358 As a result, our sub-grid representation simulates comparable surface subsidences for each sub-
359 grid landunit compared to Westermann et al. (2016), proving the reasonability of our developed
360 sub-grid representation of excess ice. We have added the above clarification in the main text
361 (Line 157-160).

362

363 6. Line 106: "The added ice is evenly distributed within each soil layer". In Figure 3, ice is not
364 depicted as evenly distributed in the cross-sectional diagrams. Tile 4 shows large ice wedges,
365 tile 3 a discontinuous (across the landunit) body of ice. The model does not represent ice in this
366 way. These diagrams should reflect that ice is evenly distributed and consistent with the
367 depictions showing "Present" and "Future" conditions.

368

369 Authors' reply: Although in the schematic figure and in reality, the ice is not distributed evenly,
370 the framework of CLM and our developed sub-grid representation is able to convert this uneven
371 distribution of excess ice into evenly-distributed excess ice landunits in the CLM. The relative

372 locations of excess ice bodies does not matter because CLM does not include horizontal heat
373 and water fluxes (we have mentioned it in the discussion section). The set-up of excess ice in
374 the CLM can be treated as “squeezing” all excess ice (of the same type) into a part of grid point
375 with evenly-distributed excess ice and the other part of the grid point without excess ice.

376

377 [References](#)

378 [French, H. and Shur, Y., 2010. The principles of cryostratigraphy. *EarthScience Reviews*,
379 *101*\(3-4\), pp.190-206.](#)

380

381 [Gilbert, G.L., O’Neill, H.B., Nemec, W., Thiel, C., Christiansen, H.H. and Buylaert, J.P., 2018.
382 Late Quaternary sedimentation and permafrost development in a Svalbard fjordâ~Rvalley,
383 Norwegian high Arctic. *Sedimentology*, *65*\(7\), pp.2531-2558. ~](#)

384

385 [Harris, S.A., French, H.M., Heginbottom, J.A., Johnston, G.H., Ladanyi, B., Seg0, D.C. and
386 Van Everdingen, R.O., 1988. Glossary of permafrost and related ground-ice terms.](#)

387

388 [Heginbottom, J.A., Dubreuil, M.A. and Harker, P.A., 1995. Canada, Permafrost. National Atlas
389 of Canada. Natural Resources Canada, 5th Edition, MCR, 4177.](#)

390

391 [Langer, M., Westermann, S., Heikenfeld, M., Dorn, W. and Boike, J., 2013. Satellitebased
392 modeling of permafrost temperatures in a tundra lowland landscape. *Remote Sensing of
393 Environment*, *135*, pp.12-24.](#)

394

395 [Schuur, E.A., McGuire, A.D., Schädel, C., Grosse, G., Harden, J.W., Hayes, D.J., Hugelius,
396 G., Koven, C.D., Kuhry, P., Lawrence, D.M. and Natali, S.M., 2015. Climate change and the
397 permafrost carbon feedback. *Nature*, *520*\(7546\), pp.171-179.](#)

398

399 [Schwamborn, G., Rachold, V. and Grigoriev, M.N., 2002. Late Quaternary sedimentation
400 history of the Lena Delta. *Quaternary international*, *89*\(1\), pp.119-134.](#)

401

402

403 Comments on “Projecting circum-Arctic excess ground ice melt with a sub-grid representation
404 in the Community Land Model” by Lei Cai et al submitted to The Cryosphere.

405

406 General

407 Permafrost soils usually contain large amount of ground ice. Its melting has significant impacts
408 on infrastructure, landscape and hydrology. Ground ice also affects the timing and speed of
409 permafrost thaw. This paper modelled the effects of ground ice on permafrost thaw using a sub-
410 grid representation in the Community Land Model. They first test the implementation in Lena
411 River delta. It shows that using three land units of different ground ice provides more realistic
412 results than using one average ice land unit. The modelled thawing depths also very different
413 among the three land units and from using the average ice content. Then they implemented the
414 representation across the circum- arctic region using four land units (no ice, low, mid and high
415 ice) and compared with the results using average ice content. The results shows more realistic
416 pathways of permafrost degradation and a different total area with permafrost comparing to
417 using average ice. The circum-arctic excess ice data are rough, the CAPS dataset is a very broad
418 generalization of the complex ground ice conditions and how to use the dataset is not
419 straightforward. However, this study does show some progress to include ground ice in a more
420 realist way than previous studies (no excess ice, or using average for an entire grid) and it
421 provides a general range of the large-scale impacts of such sub-grid differences. The paper is
422 well prepared in language and figures.

423 Authors’ reply: Thank you very much for your valuable comments. We agree that the rough
424 excess ice dataset is the main challenge when we conducted this study. Unfortunately, the
425 CAPS data is still the best excess ice data available on the global scale although it was released
426 more than 20 years ago. In this way, we have to design a tiling scheme to fit the CAPS data
427 into the sub-grid framework we developed, which is not straightforward and contains fairly
428 empirical estimates on excess ice contents and located depths. Although with the challenges on
429 the initial condition of excess ice, we manage to convey through this manuscript that a sub-grid
430 scale modeling of excess ice in the global land models is necessary for retrieving the permafrost
431 dynamics in the circum-arctic regions, and we have had the modeling tool prepared before the
432 new generation of excess ice dataset becomes available.

433

434 Major points

435 The test study shows very different active-layer thicknesses among the three land units and
436 from the one-unit with average-ice (Figure 4). The paper did not provide much about the results
437 of active-layer thickness for the circum-arctic modelling. It would be important to add this part
438 in the results and analysis. Observations on ground subsidence is sparse and highly depend on
439 the local conditions. An improved modelling of active-layer thickness would provide some
440 support evidence about the usefulness of including excess ice in sub-grids.

441 Authors’ reply: The reason we did not mention the difference of active layer depth brought by
442 the excess ice in the global case is that it is somewhat complicated because of a technical rather
443 than scientific reason. Theoretically, the presence of excess ice makes the permafrost thermal
444 regime more stable and a shallower active layer. However, it does not always show in the
445 modeling case, because the model initializes soil into discrete layers that are with different
446 thickness. For most land models, the thickness of each soil layer is not the same from top to
447 bottom. Usually, deeper soil layers are also thicker. In the original soil set-up of the CLM5, the
448 typical soil layer thickness for the depth between 0.5 to 1 meters is 0.15 meters, while that for
449 the depth between 3 to 4 meters is more than 0.5 meters. In this way, for the regions with a

450 thicker active layer (e.g. > 2 meters), the presence of excess ice is not associated with a
451 shallower active layer simply because the above soil layer is too thick (which also means the
452 chunk of soil is bigger) to make the stable thermal regime distinguishable. We have now added
453 some discussion in the main text to give readers some more insights.

454

455 “Compared to the grid average ice case, even more permafrost areas are sustained in the subgrid
456 ice case” (Line 313-314). However, Figure 9 shows the permafrost area difference between
457 sub-grid case and no ice case is similar to the difference between the average ice case and no
458 ice case before the 2050, after that the latter reached about 1 million km². That means the
459 permafrost areas under average ice case and sub-grid ice case are similar before the 2050s.
460 After that, the modelled permafrost area under average ice case is larger than under sub-grid
461 ice case. In the last two panels in Figure 7, the shaded area in the second panel seems larger
462 than the second panel. That is not consistent with the results in Figure 9. Not sure whether my
463 understanding is correct. Any way, it would be useful and interesting to provide more
464 explanation and analysis about the differences among these three cases (no ice, average ice and
465 sub grid ice).

466 Authors’ reply: In figure 9, we compared the actual area of permafrost in the sub-grid scale.
467 For example, for a certain grid point with a total area of 0.2 million km², only a landunit with
468 20% area weight has permafrost remaining (ALT <6.49 m). Then the area of permafrost for
469 this grid point is 0.02 million km². But in figure 7 and 8, we compare the permafrost
470 degradation on the grid scale. In figure 7, the complete degradation of permafrost refers to the
471 condition that all the sub-grid landunits in one grid cell are without permafrost. In figure 8, a
472 grid cell is considered “discontinuous permafrost” if some landunit has permafrost while some
473 others not. We have added more content in the figure caption to prevent misunderstandings.

474

475 The data about ground ice is rough and how to use the current data is based on some
476 assumptions or artificial choices. It would important to indicate that uncertainties more clearly
477 in the text (the paper already indicated that at different places).

478 Authors’ reply: We have added more discussion on the uncertainty because of the excess ice
479 initialization.

480

481 Minor points

482

483 Line 28-29: delete “enhance” or “improve”.

484 Authors’ reply: We have made the change as you recommended.

485

486 Lines 42-44, “The existence of excess ice and its distribution in permafrost can significantly
487 affect the rate of permafrost thawing”. It would be useful to add some references here.

488 Authors’ reply: We have added more references.

489

490 Line 58: “over generations”. It seems strange to say model versions as “generations”. It would
491 be clearer to say “in recent years” or so.

492 Authors’ reply: We have made the change as you recommended.

493

494 Line 67: “Separate from this”, revised to “In addition”

495 Authors’ reply: We have made the change as you recommended.

496

497 Line 71-74. Check the grammar for this long sentence.

498 Authors’ reply: We have checked the grammar.

499

500 Line 74-95: “the depth distribution of ground ice can vary substantially on the order to 10-50
501 meters horizontally 75 and 10 meters vertically”. Is the depth to the top of ground ice or also
502 including the thickness of ground ice? Probably you want to say both. Check and consider
503 revising the sentence.

504 Authors’ reply: Actually here we just mean the depth of ground ice rather than both the depth
505 and thickness since it is what the cited studies brought.

506

507 Line 165: “Satellite Phenology (SP) mode”, I do not know what is that. Some explanation
508 would be helpful.

509 Authors’ reply: We have had an explanation for that. SP mode means it does not involve slowly
510 evolving biogeochemical processes such as soil carbon accumulation (Line 180).

511

512 Line 220: “Have the same area fraction of low ice landunit”, You may add “(20%)” to make it
513 clearer. What is the reason behind this assumption?

514 Authors’ reply: We make this assumption based on the fact that segregated excess ice is
515 distributed widely throughout the permafrost region. So we assume that all the grid points in
516 the CAPS data have some extent of low content ice. Since we define the volumetric content of
517 excess ice in the low ice landunit as 25%, and the lowest category of excess ice in the CAPS
518 data has 5% in volumetric excess ice content, we just assume that this 5% excess ice is
519 contributed by 20% area weight of low content excess ice that is 25% in volumetric excess ice
520 content.

521

522 You must have a percentage of land as no excess ice as the total percentage is less than 100%
523 in Table 2 (e.g., for 5% CAPS, the no excess ice area would be 80%). If that is the case, it
524 would be clearer to indicate the no excess ice areal percentage in Table 2, and the scheme
525 actually uses four landunits (as shown in Figure 1) rather than three. For the grid-average ice
526 case, you used the average of the three land units (Line 242) or the four land units?

527 Authors’ reply: We have made the change in Table 2 as you recommended.

528

529 Figure 3. The legend is in km². You may provide the area of a grid or using % of the area of a
530 grid.

531 Authors’ reply: Because the grid cell with a lower latitude has a larger area. We think using
532 km² can provide more information here.

533

534 Line 259-260: “A small amount of excess ice (24kg/m²) melts during the spinup period”, which
535 case?

536 Authors’ reply: It is the average ice single-landunit case. We have added such information to
537 the sentence to make it clear.

538

539 Lines 302-303: “We define the permafrost degradation in this study as when all the landunits
540 in one grid cell has an active layer thickness greater than 6.5 meters”. That is different from the
541 sentence in line 238. Probably the sentence in lines 302-303 is for how you treat the grid in
542 figure 7. If so you can indicate its applications.

543 Authors’ reply: It is a matter of scales. In this study, only global simulation has permafrost
544 degradation condition analyzed. For figure 7 and 8, we addressed analysis on the grid scale,
545 and we regard full permafrost degradation when the permafrost in all landunit in one grid point
546 has disappeared (ALT > 6.5m). For figure 9, we addressed analysis on the landunit scale to
547 compare the actual permafrost area. In this way, we calculate the area of each landunit with
548 permafrost degraded (ALT > 6.5 m). We have reworded these sentences to make this point clear.

549

550 Line 350: “as projected until 2100”, probably revise to “as we modelled”. No observations
551 beyond present.

552 Authors’ reply: We have made the change as you recommended.

553

554 Line425, 438: “modelling”, “modelled”, be consistent with “Modeling” and “Modeled”

555 Authors’ reply: We have made the change as you recommended.

556

557

558 Projecting circum-Arctic excess ground ice melt with a sub-grid representation in the Community Land 559 Model

560 Lei Cai¹, Hanna Lee¹, Kjetil Schanke Aas², Sebastian Westermann²

561 ¹NORCE Norwegian Research Centre, Bjerknes Centre for Climate Research, 5008, Bergen, Norway

562 ²Department of Geosciences, University of Oslo, Oslo, 0315, Norway

563 *Correspondence to:* Lei Cai (leca@norceresearch.no)

564 **Abstract** To address the longstanding underrepresentation of the influences of highly variable ground ice content
565 on the trajectory of permafrost conditions simulated in Earth System Models under a warming climate, we
566 implement a sub-grid representation of excess ground ice within permafrost soils using the latest version of the
567 Community Land Model (CLM5). Based on the original CLM5 tiling hierarchy, we duplicate the natural vegetated
568 landunit by building extra tiles for up to three cryostratigraphies with different amounts of excess ice for each grid
569 cell. For the same total amount of excess ice, introducing sub-grid variability in excess ice contents leads to
570 different excess ice melting rates at the grid level. In addition, there are impacts on permafrost thermal properties
571 and local hydrology with sub-grid representation. We evaluate this new development with single-point simulations
572 at the Lena river delta, Siberia, where three sub-regions with distinctively different excess ice conditions are
573 observed. A triple-landunit case accounting for this spatial variability conforms well to previous model studies
574 for the Lena river delta and displays a markedly different dynamics of future excess ice thaw compared to a single-
575 landunit case initialized with average excess ice contents. For global simulations, we prescribed a tiling scheme
576 combined with our sub-grid representation to the global permafrost region using the dataset “Circum-Arctic Map
577 of Permafrost and Ground-Ice Conditions” (Brown et al., 1997). The sub-grid scale excess ice produces significant
578 melting of excess ice under a warming climate and enhances the representation of sub-grid variability of surface
579 subsidence on a global scale. Our model development makes it possible to portray more details on the permafrost
580 degradation trajectory depending on the sub-grid soil thermal regime and excess ice melting, which also shows a
581 strong indication that accounting for excess ice is a prerequisite of a reasonable projection of permafrost thaw.
582 The modeled permafrost degradation with sub-grid excess ice follows the pathway that continuous permafrost
583 transforms into discontinuous permafrost before it disappears, including surface subsidence and talik formation,
584 which are highly permafrost-relevant landscape changes excluded from most land models. Our development of
585 sub-grid representation of excess ice demonstrates a way forward to ~~enhance~~ improve the realism of excess ice
586 melt in global land models, but further developments rely on additional global observational datasets on both the
587 horizontal and vertical distributions of excess ground ice.

588 1. Introduction

589 Permafrost soils are often characterized by different types of ground ice that can exceed the pore space
590 (Brown et al. 1997; Zhang et al., 1999). The presence of such “excess” ground ice can alter the permafrost thermal
591 regime and landscape structure. Widespread thawing of permafrost is expected in a warmer future climate and
592 modeling studies suggest large-scale degradation of near-surface permafrost at the end of the 21st century
593 (Lawrence et al., 2008 & 2011). Melting of ground ice due to active layer thickening releases water in the form

594 of surface and/or subsurface runoff, causing surface subsidence and modifying the local hydrological cycle (West
595 and Plug, 2008; Grosse et al., 2011; Kokelj et al., 2013; Westermann et al., 2016). In addition to containing ground
596 ice, some permafrost soils store massive amounts of carbon, which could be released to the atmosphere in the
597 form of greenhouse gases upon thawing (Walter et al., 2006; Zimov et al., 2006; Schuur et al., 2008), possibly
598 making a positive feedback to amplify future climate change (Koven et al., 2011; Schaefer et al., 2014; Burke et
599 al., 2013). The existence of excess ice and its distribution in permafrost can significantly affect the rate of
600 permafrost thawing (Westermann et al., 2016; Nitzbon et al., 2020), and in turn, the rate of soil carbon release
601 (Hugelius et al., 2014; Schuur et al., 2015; Turetsky et al., 2019). Therefore, better projections of excess ice melt
602 are critical to improve our understanding of the impacts of permafrost thaw on corresponding climatic impacts.

603 Previous studies address excess ice modeling on the local or regional scale, in which the small study area
604 makes it possible for detailed configurations of the cryostratigraphy of permafrost and excess ice based on
605 observations. Simulations for the Lena river delta have retrieved the permafrost thermal dynamics fairly close to
606 the observations with excess ice incorporated in the modeling (Westermann et al., 2016). A two-tile approach
607 allowing lateral heat exchange between two land elements demonstrated that maintaining thermokarst ponds
608 requires the heat loss from water to the surrounding land (Langer et al., 2016). A similar tiling approach has been
609 applied to projecting the landscape changes due to permafrost thaw for ice-wedge polygons and peat plateaus with
610 different features of ice melting and surface subsidence (Aas et al., 2019; Nitzbon et al., 2019).

611 On the global scale, the land components of Earth System Models (ESMs) have significant capabilities of
612 representing key permafrost physics. In the Community Land Model (CLM), for example, the representation of
613 permafrost-associated processes has been continuously improving over generations. By including key thermal
614 and hydrological processes of permafrost, the CLM version 4 (CLM4) has reasonably reproduced the global
615 distribution of permafrost (Lawrence et al., 2008; Lawrence et al., 2012; Slater and Lawrence, 2013). Projections
616 based on the CLM4 under its highest warming scenario (RCP8.5) have shown over 50% degradation of near-
617 surface permafrost by 2100 (Lawrence et al., 2012). Moreover, the recently released CLM5 has more advanced
618 representations of many biogeophysical and biogeochemical processes (Lawrence et al., 2019). A refined soil
619 profile and upgraded snow accumulation and densification scheme in the CLM5 could contribute to simulating
620 more realistic permafrost thermal regimes, whereas upgrades on biogeochemistry improve simulations of soil
621 carbon release in response to permafrost thaw. In addition~~Separate from this~~, an excess ice physics scheme has
622 been implemented in CLM4.5 (CLM4.5_EXICE) by Lee et al. (2014), which allowed for the first-order simulation
623 of surface subsidence globally by modeling excess ice melt under a warming climate.

624 The homogeneous distribution of excess ice throughout the grid cell in CLM4.5_EXICE (Lee et al., 2014)
625 could cause biases in thaw trajectories in the warming climate. In nature, excess ice forms in a highly localized
626 manner due to a variety of accumulation processes. For instance, segregated ice formed during frost heave differs
627 substantially in excess ice morphology from ice wedges that are formed from repeated frost cracking and freezing
628 of penetrating water. Field measurements illustrate that the depth distribution of ground ice can vary substantially
629 on the order to 10-50 meters horizontally and 0-10 meters vertically (Pascale et al., 2008; Fritz et al., 2011). The
630 horizontal grid spacing of ESMs, on the other hand, usually ranges from one to two degrees (~100-200km
631 horizontal scale), which makes it impossible to represent localized excess ice. The mismatch in spatial scale

632 between model and the real world raises concerns for the reliability of excess ice modeling in ESMs. Aside from
633 the homogeneously-initialized excess ice in the grid cell, CLM4.5_EXICE initializes excess ice in the same soil
634 depths globally (below 1m), regardless of the varying active layer thickness in circum-Arctic permafrost areas
635 (Lee et al., 2014). Such deficiencies in excess ice parameterization hamper global projections of permafrost thaw
636 including excess ice with ESMs.

637 To narrow the gap between the high spatial variability of excess ice and the coarse grid spacing in the ESMs,
638 we applied a sub-grid approach in representing excess ice in permafrost soils within the CLM5 to investigate how
639 presence and melting of excess ice affect land surface physics under a warming climate. We conducted idealized
640 single-point simulations to examine the robustness of model development. We furthermore conducted global
641 simulations using a first-order estimate for the spatial distribution of excess ice and associated cryostratigraphies,
642 aiming to present a model framework that can eventually bring the modeling ~~We furthermore conducted global~~
643 ~~simulations using a prescribed set of sub-grid scale excess ice conditions, aiming to bring the modeling of excess~~
644 ~~ice melt and the corresponding impacts on the global scale~~ towards a higher accuracy. Due to the lack of
645 information in global excess ice conditions, it is not the aim of this study to accurately project excess ice melt and
646 surface subsidence in the 21st century, but rather to develop a functional process within a land surface model
647 on a global scale. The CLM5 with sub-grid excess ice representation developed through this study would be ready
648 to serve as a proper simulation tool on further advancing global excess ice modeling once new datasets become
649 available.

650 **2. Methodology**

651 **2.1 Sub-grid representation of excess ice in the CLM5**

652 The CLM5 model utilizes a three-level tiling hierarchy to represent sub-grid heterogeneity of landscapes,
653 which are (from top to bottom) landunits, columns, and patches (Lawrence et al., 2019). There is only one column
654 (the natural soil column) that is under the natural vegetated landunit, which represents soil including permafrost.
655 In this study, we modify the CLM5 tiling hierarchy by duplicating the natural vegetated landunit, making extra
656 landunits for prescribing up to three different excess ice conditions in permafrost (Figure 1). The original natural
657 vegetated landunit is considered as “natural vegetated with no excess ice” (hereafter no ice landunit), while we
658 denote the additional landunits as “natural vegetated with low content of excess ice” (hereafter the low ice
659 landunit), “natural vegetated with medium content of excess ice” (hereafter the mid ice landunit), and “natural
660 vegetated with high content of excess ice” (hereafter the high ice landunit). The sub-grid initial conditions of
661 excess ice are imported as part of the surface data, which includes the variables of volumetric excess ice contents,
662 depths of the top and bottom soil layer of added excess ice, and the area weights of the four landunits.

663 We adopted the excess ice physics from CLM4.5_EXICE (Lee et al., 2014), including thermodynamic and
664 hydrological processes. The added excess ice is evenly distributed within each soil layer. Note that the original
665 CLM5 model already represents the dynamics of pore ice. Our representation of excess ice physics only addresses
666 the ground ice bodies that exceed soil pore space. The volumetric excess ice content in this study is defined as the
667 ratio of the volume of excess ice in a soil layer to the volume of the whole soil layer. For example, a 50%

668 volumetric content of excess ice means the excess ice body occupies 50% volume of a soil layer, while the rest of
669 soil (and pore ice) occupies the other 50% volume of the soil layer. If not otherwise notified, the parameter of
670 volumetric ice content in this manuscript refers only to that of excess ice bodies. After adding excess ice, the soil
671 layer thickness increases accordingly. Because ice density is considered constant, the increase of soil layer
672 thickness is linearly proportional to the volumetric content of excess ice. For example, adding an excess ice body
673 with a 50% volumetric excess ice content doubles the soil layer thickness of the corresponding soil layer. The
674 revised algorithm for thermal conductivity and heat capacity of soil involves the effects of added excess ice, while
675 the revised phase change energy equation allows excess ice to melt. The meltwater adds to soil liquid water in the
676 same soil layer, and it can move to the above layer if the original layer is saturated. Such numerical implementation
677 replicates how the melt excess ice eventually converts to runoff and discharges from the soil in case of well-
678 drained conditions. As excess ice melts, soil layer thickness decreases, which corresponds to surface subsidence
679 due to excess ice melt. In our model parameterization, excess ice only melts and does not re-form since the applied
680 excess ice physics does not account for the different ice formation processes.

681 Aside from sub-grid tiles for excess ice, we acknowledge that the version upgrade from CLM4.5 to CLM5
682 as the base model modifies the results of excess ice melt compared to the results from Lee et al. (2014). By default,
683 CLM5 represents soil with a 25-layer profile, for which the top 20 hydrologically-active layers cover 8.5 meters
684 of soil. There are additional 10 soil layers and it is 4.7 meters deeper compared to the default hydrologically-active
685 soil layer profile in CLM4.5, not to mention the substantially more complex biogeophysical processes (Lawrence
686 et al., 2019). Therefore, we developed the sub-grid representation of excess ice within the framework of the latest
687 version of CLM. The duplicated landunits prolong computation time by roughly 10% compared to the original
688 CLM5. We are, therefore, confident that our model development is highly efficient in addressing the sub-grid
689 excess ice and subsequent permafrost thaw.

690 **2.2 Single-point simulations for the Lena river delta, Siberia**

691 We conduct single-point simulations for the Lena River delta and compare the CLM5 model results to
692 reference simulations with the CryoGrid3 model for the same location (Westermann et al., 2016). Abundant
693 background information is available on the soil and ground ice dynamics from both observation and modeling,
694 making the Lena river delta a suitable location to further evaluate our model development. The Lena river delta
695 can be broadly categorized into three different geomorphological units that have distinctively different subsurface
696 cryostratigraphies of excess ice (Schneider et al., 2009; Ulrich et al., 2009). In the eastern and central part of the
697 river delta, ground ice has been accumulated in the comparatively warm Holocene climate. The subsurface
698 sediments (hereafter denoted as “Holocene ground ice terrain”) are generally super-saturated with wedge ice that
699 can extend up to 9 meters underground with the volumetric ~~ice~~-contents of total ground ice (pore ice + excess ice)
700 ranging from 60-80% (Schwamborn et al., 2002; Langer et al., 2013). On the other hand, higher excess ice contents
701 are found in Pleistocene sediments in the Lena River Delta (hereafter the “Yedoma Ice complex”), which are
702 characterized by Yedoma type ground ice (Schirrmeister et al., 2013), which can reach depths of up to 20-25
703 meters deep and volumetric contents of total ground ice~~volumetric ice contents as high as 90%~~ (Schwamborn et
704 al., 2002; Schirrmeister et al., 2003 and 2011). Finally, the Northwestern part of the delta features sandy sediments
705 and is characterized by low excess ice contents (hereafter denoted the “no excess ice terrain”; Rachold and

706 Grigoriev, 1999; Schwamborn et al., 2002).

707 We determine the area weights of excess ice landunits in one single point based on the spatial pattern of three
708 subregions (Fedorova et al., 2015). The cryostratigraphy and ~~the volumetric contents of excess ice~~
709 ~~contents~~ strictly follow those in Westermann et al. (2016). Note that the excess ice initialization scenario in
710 Westermann et al. (2016) does not necessarily represent the realistic excess ice condition for the Lena river delta.
711 The purpose of applying the same excess ice cryostratigraphy as in Westermman et al. (2016) is to evaluate our
712 model development by addressing intercomparisons between model results. Meanwhile, we did not customize soil
713 properties for different landunits as in Westermann et al. (2016), as our model development does not support
714 varying soil properties for different sub-grid landunits. We also directly apply the snow accumulation physics in
715 the CLM rather than customizing the snow density. By default, the current model does not form thermokarst lakes
716 as the meltwater from excess ice melt becomes surface runoff and is removed from the grid cell. To apply the sub-
717 grid representation, we initialize the case with three landunits (the triple-landunit case) that respectively represent
718 the three terraces in the Lena river delta. We also initialize an “average ice single-landunit” case without the sub-
719 grid representation of excess ice. The excess ice amount for each soil layer in the average ice single-landunit case
720 is initially the same as that in the triple-landunit case. The volumetric-~~ice~~ content of excess ice is determined by
721 spatial averaging those for three excess ice landunits in the triple-landunit case. Detailed information on the
722 applied excess ice conditions for both cases is listed in Table 1.

723 We employed the single-point forcing data from in Westermann et al. (2016) for the Lena river delta from
724 1901 to 2100, which is based on the CRU-NCEP (<http://dods.extra.cea.fr/data/p529viov/cruncep/>) data set for the
725 historical period (1901-2005) and the CCSM4 model output under the RCP4.5 scenario for the projected period
726 (2006-2100), but downscaled with in-situ observations. We run 100-year spin-up simulations in order to stabilize
727 the permafrost thermal regime after adding excess ice. Spin-up simulations are produced by running the model
728 with cycled 1901-1920 climatological data. The purpose of spin-up simulations is to stabilize ground temperatures
729 and volumes of excess ice bodies. The 100-year length for spin-up is sufficient, as the model is run in Satellite
730 Phenology (SP) mode that does not involve slowly evolving biogeochemical processes such as soil carbon
731 accumulation. Moreover, we address idealized single-point simulations for additional permafrost locations with
732 both continental and maritime climate that showcase the difference to Lee et al. (2014), the results of which are
733 included in the Supplementary material.

734 **2.3 Global simulations of excess ice melt**

735 The information available for the spatial distribution of excess ice and associated cryostratigraphies on the
736 global scale is generally not as detailed as in the Lena river delta due to the lack of observations. For our global
737 simulations we employ the widely used “Circum-Arctic Map of Permafrost and Ground-Ice Conditions” (hereafter
738 the CAPS data; Brown et al., 2002) as data source, while we translate the ground ice condition in the CAPS data
739 to different excess ice stratigraphies as model input data. The CAPS permafrost map categorizes the global
740 permafrost area into classes coded by three factors (i) permafrost extent (c = continuous, d = discontinuous, s =
741 sporadic, and i = isolated), (ii) visible ground ice content (h = high, m = medium, and l = low), and (iii) terrain
742 and overburden (f = lowlands, highlands, and intra- and intermontane depressions characterized by thick
743 overburden cover, and r = mountains, highlands ridges, and plateaus characterized by thin overburden cover and
744 exposed bedrock), resulting in more than 20 different varieties in permafrost characteristics (Figure 2). For the

745 simulations, we only use the CAPS distinction between the three classes: high, medium and low ice contents. We
746 qualitatively categorize excess ice types with typical cryostratigraphies for which observations are available,
747 recognizing that this is a crude first-guess of the global distribution of ground ice which needs to be improved
748 in future studies.

749 The high ice CAPS classes (e.g. chf, chr, and dhf) in central and eastern Siberia, as well as in Alaska, partly
750 coincide with Yedoma regions (Kanevskiy et al., 2011; Grosse et al., 2013). The cryostratigraphy of the high ice
751 landunit is therefore broadly oriented at the excess ice contents and distribution in intact Yedoma, which is
752 characterized by massive ice wedges leading to typical average volumetric content of total ground ice in the range
753 from 60% to 90% (Schwamborn et al., 2002; Kanevskiy et al., 2011). We therefore set the volumetric ~~excess ice~~
754 content of excess ice in the high ice landunit to 70%, and we put excess ice in all the soil layers between 0.2 meters
755 below the active layer and the bottom of hydrologically-active soil layer (8.5 meters). The onset depth of the
756 excess ice just below the active layer is based on the assumption of active ice aggradation which occurs at or
757 below the permafrost table, e.g. the formation of wedge or segregation ice. Initializing high content excess ice
758 throughout the whole soil layer imitates the cryostratigraphy of Yedoma type ice, while a certain amount of high
759 ice landunit locates out of the observed Yedoma regions (Schuur et al., 2015). The effects, limitations, and
760 potential improvements of this initialization scenario will be mentioned in the discussion section. For the low ice
761 landunit, we assume both a significantly lower volumetric ~~excess~~ ice content and a smaller vertical extent of the
762 excess ice body. The volumetric excess ice content is set to 25%, and we add excess ice at soil layers within 0.2
763 to 1.2 meters below the active layer, which in particular represents sediments with segregated ice (e.g. Cable et
764 al., 2018), but also accounts for a wide range of different excess ice conditions found throughout the permafrost
765 domain. For the mid ice landunit, we set the volumetric excess ice content to 45% and put excess ice within 0.2
766 to 2.2 meters below the active layer, making the volumetric ~~excess~~ ice content and vertical extent of which in
767 between those for the low and high ice landunits. The cryostratigraphies determine that excess ice melt in the low
768 ice landunit can result in a maximum of 0.36 meters of surface subsidence, while excess ice melt in the medium
769 ice landunit can result in a maximum of 1.78 m of surface subsidence. For the high ice landunit, the surface
770 subsidence can be more than 10 meters if all excess ice melts, which is expected to vary in space because of the
771 different active layer thickness. For all three landunits, the active layer thickness is determined by the soil
772 temperature profile by the end of the spinup in a no ice case, which is the simulation by the original CLM5 model
773 without excess ice incorporated. Non-permafrost regions in the CAPS data are assigned the no ice landunit for
774 100% of their area. We emphasize that the prescribed cryostratigraphies are a coarse first-order approximation
775 that can by no means represent the wide variety of true ground ice conditions found in the permafrost domain.
776 Nevertheless, this makes it possible to gauge the effect of excess ice melt on future projections of the permafrost
777 thermal regime, when compared to “traditional” reference simulations without excess ice.

778 We design a tiling scheme prescribing the assignment of landunits for each CAPS class based on previous
779 observations and empirical estimates (Table 2). All CAPS classes in this study are categorized into three levels of
780 volumetric ice content (5%, 15%, and 25%) that are converted from the ranges (<10%, 10-20%, and >20%) in the
781 original CAPS data. The goal of our tiling scheme is to determine a combination of area weights of three excess
782 ice landunits for each CAPS class, making the spatially averaged volumetric ~~ice~~ content of excess ice the same as
783 that for the CAPS class. We assume that all CAPS classes have the same area fraction (20%) of the low ice landunit,

784 and the CAPS classes with a higher ice content are due to the existence of the landunits with a higher content
785 excess ice. We make this assumption based on previous studies that the segregated ice is widely distributed in
786 permafrost. Observational studies have found segregated ice bodies in various continuous permafrost regions
787 across the circum-arctic including West Central Alaska (Kanevskiy et al., 2014), Nunavik, Canada (Calmels and
788 Allard, 2008), and Svalbard (Cable et al., 2018). In discontinuous permafrost regions, segregated ice bodies also
789 commonly exist underneath Palsas and Lithasas, including Fennoscandia (Seppälä, 2011), Altai and Sayan, Russia
790 (Iwanhaha et al., 2012), Himalayas (Wünnemann et al., 2008), and Mongolia (Sharkhuu et al., 1999). The
791 volumetric content of visible segregated ice bodies mentioned above ranges widely from 10-50% (Gilbert et al.,
792 2016).

793 Given the tiling scheme~~ice content~~ prescribed above, all CAPS classes are assigned a 20% area of low ice
794 landunit. Correspondingly, the CAPS classes with 15% volumetric ice content are assigned another 14% area
795 weight for mid ice landunit on top of the CAPS classes with 5% volumetric ice content, while the CAPS classes
796 with 25% volumetric ice are assigned another 22% area for high ice landunit on top of the CAPS classes with 15%
797 volumetric ice content. The classes of “chf” and “chr” are the exceptions as their corresponding regions are
798 typically with the landscape of Yedoma and/or ice wedge polygonal tundra (Kanevskiy et al., 2011; Gross et al.,
799 2013). We therefore assign only the low and high ice landunits for these two CAPS classes. Summing up the
800 landunit fractions for all the CAPS grid cells within each CLM grid cell obtains the area weights on the grid level
801 that are stored in the surface data file. Figure 3 shows a schematic plot for the initialization scenario and the area
802 covered by different excess ice landunits as the result of sub-grid excess ice initialization in the global simulation
803 case. Note that excess ice for some regions (e.g. Southern Norway and the Alps) can completely melt out during
804 the spinup period since the CLM initial condition prescribes overly warm (non-permafrost) soil temperature for
805 these regions.

806 In this study, we define the grid cells/landunits with permafrost as the ones having at least one hydrologically
807 active soil layer that has been frozen in the last consecutive 24 months. In this case, we define permafrost
808 degradation when all landunits in one grid point are degraded~~permafrost as permafrost landunits~~ with active layer
809 thickness more than 6.5 meters. We also prepare a “grid-average ice case” by applying the same total amount of
810 excess ice as in the sub-grid ice case in each soil layer, but using only one landunit instead of three that account
811 for the sub-grid variability of excess ice. The volumetric ~~excess ice content~~ of excess ice in the single landunit is
812 calculated as the spatial average of those in the three landunits in the triple-landunit case. This grid-average ice
813 case provides a reference to evaluate the effects of the sub-grid excess ice representation on the global scale.
814 Finally, we simulate a reference case without excess ice, denoted the “no ice case” in the following. Details on the
815 three cases for the global simulations are listed in Table 3. All global cases are forced by the 3rd version of Global
816 Soil Wetness Project forcing data (GSWP3; Kim et al., 2012), running in the Satellite Phenology (SP) mode. The
817 International Land Atmosphere Model Benchmarking (ILAMB; Collier et al., 2018) project has indicated the
818 superior performance of GSWP3 data forcing the CLM5 in the SP-only mode
819 (http://webext.cgd.ucar.edu/I20TR/_build_090817_CLM50SPONLY_CRUNCEP_GSWP3_WFDEI/index.html).
820 We conducted a 100-year spin-up using the 1901-1920 climatology before conducting historical period
821 simulations covering 1901-2005. The anomaly forcing under the RCP8.5 scenario on top of the 1982-2005
822 climatology forces simulations in the projected period.

823 3. Result

824 3.1 Excess ice melt simulations for Lena River delta cryostratigraphies

825 By the end of the spinup in the triple-landunit case, the active layer thickness is 0.85 m, 0.55 m, and 0.45 m
826 for the ice-poor terrain, the Holocene ice wedge terrain, and the Yedoma ice complex, respectively. On the other
827 hand, the active layer thickness for the average ice single-landunit case is 0.85 m, which is the same as in the no
828 excess ice terrain in the triple-landunit case. [For the average ice single-landunit case, a](#) small amount of excess
829 ice (24kg/m^2) melts during the spinup period, resulting in 2.6 cm surface subsidence throughout the grid.

830 For the Yedoma ice complex, very little excess ice melt in the 1950s, and it stabilizes afterwards until the late
831 2000s when substantial ice melt and surface subsidence starts to happen. For the Holocene ground ice terrain,
832 there is no excess ice melt before the late 2010s. By the year 2100, the Yedoma ice complex has exhibited nearly
833 4 meters of surface subsidence, while the Holocene ground ice terrain has about 0.6 meters of surface subsidence
834 (Figure 4). For the average ice single-landunit case, the noticeable excess ice melt and surface subsidence starts
835 in the late 2010s, which creates about 0.5 meters of surface subsidence by 2100. The magnitude of surface
836 subsidence in the average ice single-landunit case is lower than both the Holocene ground ice terrain and the
837 Yedoma ice complex in the triple-landunit case.

838 On the grid scale, the total excess ice melt is higher in the average ice single-landunit case than in the triple-
839 landunit case (Figure 5). By the year 2100, the average ice single-landunit case has about 30 kg/m^2 more excess
840 ice melt than the triple-landunit case. The difference in excess ice on the grid level results from the different
841 volumetric ~~ice~~-content [of excess ice](#) caused by the spatial averaging. In this way, the sub-grid representation of
842 excess ice can potentially also provide more detailed and realistic representation of model variables on the grid
843 level. This is particularly important for the CLM5, which serves as the land component in Earth System Models,
844 which requires the coupling between interacting components on the grid level.

845 Compared to Westermann et al. (2016), the CLM5 with sub-grid excess ice simulates slightly less ($\sim 20\%$
846 less) surface subsidence by 2100 for both the central delta and ice complex. We consider this a good agreement
847 as we do not expect a closer fit of the model results due to substantial differences in the model physics (for example,
848 the Cryogrid3 simulations in Westermann et al. (2106) lack a representation of the subsurface water cycle). What
849 is in common between these two studies is the earlier start of excess ice melt and more surface subsidence in the
850 ice complex than in the central delta. The CLM5 with sub-grid excess ice also exhibits the varying active layer
851 thickness with different excess ice conditions as Cryogrid3 does. These results suggest that the new model
852 development enables small-scale variability in excess ice melt and subsequent impacts in agreement with
853 previously published modeling efforts.

854 3.2 Global projection of permafrost thaw and excess ice melt

855 Single-point simulations have shown that the varying excess ice cryostratigraphies for different landunits
856 result in sub-grid variabilities of excess ice melt and surface subsidence under the warming climate. The same
857 features remain in the sub-grid ice case within the global simulations that excess ice in the low ice landunit can
858 completely melt out throughout the circum-Arctic permafrost region by the end of the 21st century (Figure 6). The
859 modeled magnitude of surface subsidence is similar to the $\sim 10\text{ cm}$ surface subsidence observed in Barrow and
860 West Dock in the early 21st century (Shiklomanov et al., 2013; Streleskiy et al., 2017). The magnitude of surface

861 subsidence is also comparable to the 1-4 cm decade⁻¹ surface subsidence rate on average over the North Slope of
862 Alaska observed by satellite measurements since the 1990s (Liu et al., 2010). In comparison, the absence of
863 surface subsidence for Arctic Alaska modeled by Lee et al. (2014) is due to an overly deep (1 m deep) excess ice
864 initialization depth. By the year 2100, most ice in the medium ice landunit melts away in the sub-arctic region,
865 while there is less ice melt in the colder regions such as the North Slope of Alaska and the central Siberia. The
866 high ice landunit has the greatest surface subsidence among the three because of its high excess ice content, leading
867 to 2-5 meters of surface subsidence by the year 2100.

868 The existence of excess ice modulates the thermal regime of permafrost soil and is a major control on
869 permafrost degradation trajectories in a warming climate. ~~We define the permafrost degradation in this study as~~
870 ~~when all the landunits in one grid-cell has an active layer thickness greater than 6.5 meters.~~ Permafrost with excess
871 ice consistently exhibits delayed permafrost degradation compared to the no ice case (Figure 7). For the no ice
872 case modeled by the original CLM5, more than half of the permafrost area undergoes degradation by the end of
873 the 21st century. By 2100, the only areas where permafrost remains are the North Slope of Alaska, Northern Canada,
874 and the majority of the land area in Northern Siberia. The areas with remaining permafrost in the year 2100 under
875 the RCP8.5 scenarios are substantially larger compared to the CLM4 simulations, in which nearly all permafrost
876 in Eurasia becomes degraded (Lawrence et al., 2012). For the grid-average ice case, the presence of excess ice
877 stabilizes the permafrost thermal regime and thus sustains a larger permafrost area on a global scale in the
878 simulation. For example, permafrost areas in some subarctic regions in the eastern and western Siberia, as well as
879 part of the Arctic coastal regions in Yukon Territory, Canada, remain in the grid-average ice case by 2100.
880 Compared to the grid-average ice case, even more permafrost areas are sustained in the sub-grid ice case, most of
881 which are located in southern Siberia. In the subarctic regions in Alaska and Northwest Canada as well as part of
882 the central Siberia, permafrost degradation is delayed from the 2040s in the grid ice case to the 2080s in the sub-
883 grid ice case. We emphasize that permafrost is only sustained according to the accepted temperature-based
884 definition (ground material at temperature below zero for two consecutive years), but excess ice continuously
885 melts in this process, which energetically is a different mode of permafrost degradation, similar to a negative mass
886 balance of glaciers and ice sheets.

887 In the sub-grid ice case, the landunits with high excess ice contents lead to more grid points for which
888 permafrost conditions remain in the year 2100 compared to the grid-average ice case. On the other hand,
889 permafrost with excess ice only covers a fraction of a grid point. Among the permafrost degradation trajectories
890 in the three global simulation cases (Figure 8), the sub-grid ice case can provide a more detailed picture on the
891 timing of permafrost degradation. Grid cells become ‘partially degraded permafrost’ if landunits with excess ice
892 still contain permafrost, which phenomenologically is a more realistic representation that also makes it possible
893 to represent the permafrost distribution in the discontinuous and sporadic permafrost zones. On the other hand,
894 only “fully degraded permafrost” and “remaining permafrost” can be distinguished for the no ice and grid-average
895 ice case. Under the warming climate in the 21st century, the existence of excess ice, especially the high content of
896 excess ice, has a stabilizing effect on soil temperature that delay the disappearance of permafrost on the sub-grid
897 level. Therefore, by the year 2100, there are regions with partially degraded permafrost in between intact and
898 degraded permafrost (Figure 8). For example in western Siberia, the Pacific coastal area of eastern Siberia,
899 Northwestern Canada, and along the Brooks Range in Alaska, taliks form for landunits with low excess ice
900 contents which leads to partially degraded permafrost regions. Therefore, permafrost degradation exhibits a

901 gradual transition from continuous to discontinuous permafrost, and to non-permafrost regions. Some of these
902 regions also encounter substantial surface subsidence in the high ice landunit (> 5 m) (Figure 6).

903 We further compare the total permafrost area (defined as landunits with active layer thickness < 6.5 meters)
904 in the three cases throughout time. The differences in permafrost area increase from the grid-average ice case and
905 sub-grid ice case to the no ice case at a rate of 1000 km² per year until 2050 (Figure 9). After 2050, the area
906 difference of permafrost in the grid-average ice case and no ice cases rapidly increases, which reaches nearly one
907 million km² by 2100. In the sub-grid ice case, the rate of increase remains relatively unchanged after 2050,
908 resulting in an about 0.2 million km² larger permafrost area than that in the no ice case.

909 4. Discussion

910 The aim of the sub-grid excess ice representation in the CLM5 is to facilitate long-term global projection of
911 excess ice melt and surface subsidence in the permafrost regions, but the corresponding observational data for
912 model evaluation is sparse, considering especially that drastic excess ice melt as ~~modeled~~projected until 2100 is
913 only observed in few locations today (e.g. Günther et al., 2015). In the following, we discuss the challenges and
914 limitations of the sub-grid excess ice framework, and how this sub-grid representation can potentially help the
915 development of other CLM components.

916 Both single-point and global test simulations in this study have shown that excess ice melts under a warming
917 climate is sensitive to its initialization depth. The active-layer-dependent excess ice initialization in this study in
918 the global simulation (sub-grid excess ice case) yields excess ice melt and surface subsidence rates in the early
919 2000s that are comparable to observations. The lower depths of the assumed excess ice body controls the
920 termination of excess ice melt which at the same time determines the onset of talik formation in many permafrost
921 areas. Due to the scarcity of observational data, it is unclear to what extent the cryostratigraphies assumed in our
922 tiling scheme can reproduce the true vertical extent of excess ice bodies at least in a statistical sense. Even so, we
923 manage to make the prescribed excess ice condition as close to the previous results as possible. Firstly, our tiling
924 scheme on the large scale strictly follows the CAPS data (Brown et al., 2002) in terms of the volumetric excess
925 ice content. Furthermore, statistics by Zhang et al. (2000) suggest the ranges of the vertical extent of ice-rich
926 permafrost of 0-2 meters and 2-4 meters respectively for the CAPS classes with low (5%) and medium (15%) ice
927 content. Comparatively, the vertical extents permafrost with excess ice prescribed by our tiling scheme are
928 respectively 1.36 meters and 3.78 meters for the same CAPS classes, both of which lie within the ranges in Zhang
929 et al. (2000). The vertical extent of ice-rich permafrost for the high ice landunit is much higher than that (4-6
930 meters) in Zhang et al. (2000), but the unmelted part of the ice bodies does not strongly affect the overall rate of
931 excess ice melt, although the remaining ice can slightly change soil temperature and moisture of the surrounding
932 permafrost. We therefore imply that our high ice landunit initialization would not induce a strong bias in excess
933 ice melt projection in the 21st century.

934 Due to the lack of excess ice datasets and observational evidence, the excess ice initialization scenarios in
935 the global simulation cases involve empirical estimates and simplifications, which could bring biases to the
936 projection of excess ice melt and surface subsidence. We apply the volumetric content of ground ice in the CAPS
937 data approximately as the volumetric content of excess ice during initialization as the CAPS data is mostly based

938 ~~on visible ice bodies (Heginbottom et al., 1995), not to mention the determination of volumetric contents of excess~~
939 ~~ice for three landunits also result from sparse observations and empirical estimates.~~ The prescribed ~~excess ice~~
940 ~~cryostratigraphies~~ ignores ~~ice morphology and possible-the~~ variations of ~~volumetric content of excess ice~~
941 ~~content~~ with soil depth, ~~regarding initializing~~ excess ice as ~~homogeneous~~ “ice cubes” ~~with a homogeneous ice~~
942 ~~content.~~ For the high ice landunit, we simplify the cryostratigraphy initialization to Yedoma type ice, which
943 ~~prescribes overly thick excess ice bodies out of the Yedoma regions (Schurr et al., 2015). A deficiency in the~~
944 ~~current version of source code disables us to initialize non-Yedoma wedged ice for the high ice landunit out of the~~
945 ~~Yedoma region. Future versions of our model development will have more freedom in excess ice stratigraphy~~
946 ~~configuration, which makes it possible to prescribe different cryostratigraphies of the same landunit (e.g. the high~~
947 ~~ice landunit) for different locations. Furthermore, excess ice stratigraphy~~ We simplify the ~~excess ice~~ content
948 ~~initialization for two reasons. Firstly, the model development serves the land component of an earth system model~~
949 ~~that focuses on large-scale changes. Furthermore, there is not enough observational evidence for us to prescribe~~
950 ~~the variability of excess ice content with geographic locations and soil depths. Because of~~ Due to ~~Because of~~ the
951 ~~above-such~~ shortcomings in the excess ice initialization, we do not expect the modeled excess ice melt in this
952 study to be an adequate representation of reality yet, ~~whilebut~~ improved observational data sets of excess ice
953 contents and cyostratigraphies could be directly ingested to yield improved results. ~~Our model development is~~
954 ~~capable of supporting three different excess ice landunits for each grid point, but the cryostratigraphies assumed~~
955 ~~in the initialization in principle also vary in space.~~ However, ~~at present~~, a spatially distributed global dataset with
956 quantitative information on excess ice stratigraphies does not exist ~~at present~~. We emphasize that for a better
957 projection of excess ice melt, more observational data of excess ice distribution and surface subsidence is required
958 to further evaluate and validate the new model implementation of excess ice. On the regional scale, Jorgenson et
959 al. (2008) presented a permafrost map of total ground ice volume for the uppermost 5 meters of permafrost based
960 on both observations and estimates for Alaska. In addition, O’Neill et al. (2019) compiled permafrost maps for
961 Northern Canada by paleographic modeling, mapping the abundances of three types of excess ice respectively.
962 Further improvements of model results ~~dependare-dependent~~ on additional observationally constrained datasets
963 of excess ice conditions on the global scale.

964 The area weights of the excess ice landunits (Table 2) in the global simulation are obtained from the higher-
965 resolution CAPS points located within a CLM grid cell. However, complex landscape development, such as
966 thermokarst ponds, requires knowledge of the meter-scale distribution, for example the extent and geometry of
967 individual ice wedges (Langer et al., 2016; Nitzbon et al., 2019), which cannot be represented with the still coarse-
968 scale excess ice classes from the CAPS map. One possible solution to represent this could be to include another
969 layer of sub-grid tiles below the CLM landunit level, where the individual tiles can interact laterally. This would
970 allow for the representation of small-scale permafrost features within a large-scale landunit with a given excess
971 ice content. An example of how this could work is given by Aas et al. (2019) who simulated both polygonal tundra
972 and peat plateaus with a two-tile interactive setup. This is also similar to the recent representation of hillslope
973 hydrology by Swenson et al. (2019), where sub-grid tiles (on the column level in CLM) were used to represent
974 different elements in a representative hillslope. In the future development of CLM, this could be part of a more
975 generic tiling system where lateral heat and mass fluxes could be switched on and off to represent a wide range
976 of land surface processes that are currently ignored or parameterized in LSMs. Fisher and Koven (2020) have
977 discussed the challenges and opportunities in such an adaptive and generic tiling system. We would also advocate

978 for enhancing current tiling schemes in such a direction, which could substantially improve the realism in the
979 representation of permafrost landscapes in LSMs. However, the success of such a tiling approach will rely heavily
980 on the availability of adequate observational data, further highlighting the need for observational efforts and close
981 collaboration between field scientists and modelers.

982 The more detailed simulation of permafrost degradation trajectory with a sub-grid representation of excess
983 ice also builds more potential on better modeling the permafrost-carbon feedback with biogeochemistry activated
984 (CLM5BGC). Excess ice stabilizes the permafrost thermal regime, therefore alter the rate of carbon releasing from
985 the permafrost (Shuur et al., 2008). Improved projections of permafrost warming could also enhance modeling of
986 vegetation type changes (e.g. shrub expansion) that determines the nitrogen uptake to the atmosphere (Lorant
987 and Goetz, 2012). On the other hand, the possibility to simulate surface subsidence and excess ice meltwater
988 formation also opens the possibility of a more accurate representation of wetland formation. The increase in the
989 area of wetland and soil moisture have an impact of the balance of CH₄ and CO₂ releasing from the permafrost as
990 more organic matter could decompose in an anaerobic pathway (Lawrence et al., 2015; Treat et al., 2015).
991 Compared to the parameterized inundated area simulation in the CLM5 (Ekici et al., 2019), a process-based
992 wetland physics scheme together with the sub-grid representation of excess ice in this study would substantially
993 contribute to the biogeochemical modeling over the circum-arctic area.

994 **5. Conclusion**

995 This study develops a sub-grid representation of excess ice in the CLM5 and examines the impacts of the
996 existence and melting of excess ice in the sub-grid scale in a warming climate. Extra landunits duplicated from
997 the natural vegetated landunit in the CLM sub-grid hierarchy make it possible to prescribe up to three different
998 excess ice conditions in each grid point with permafrost.

999 A test over the Lena river delta showcases that the sub-grid representation of excess ice can retrieve the sub-
1000 grid variability of annual thaw-freeze state and the excess ice melt/surface subsidence through time. On the other
1001 hand, initializing excess ice homogeneously throughout the grid cell produces a smaller stabilization effect of
1002 excess ice to the permafrost thermal regime and the local surface subsidence under a warming climate. With a
1003 tiling scheme ingesting a global data set of excess ice condition into the CLM surface data, our model development
1004 shows the capability of portraying more details on simulating permafrost degradation trajectories. As excess ice
1005 thermally stabilizes the permafrost on the sub-grid scale, permafrost degrades with a trajectory from continuous
1006 permafrost to discontinuous permafrost, and finally to a permafrost-free area. The modeled global pattern of
1007 permafrost therefore exhibits regions of discontinuous permafrost as the transition zone between the continuous
1008 permafrost and degraded permafrost.

1009 This study, for the first time, used an ESM to project excess ice melt/surface subsidence and permafrost
1010 degradation with sub-grid variability. The approach of duplicating tiles at the landunit level instead of the column
1011 level allows more freedom for further developments in this direction. Furthermore, the new CLM tiling hierarchy
1012 has much more potential than representing more accurate excess ice physics as examined in this study. Further
1013 advancing the excess ice modeling relies on additional observational studies/datasets of the excess ground ice
1014 conditions on a global scale. The model development in our study, therefore, lays the foundation for further

1015 advances focusing on excess ice modeling and other processes in the CLM framework that could benefit from an
1016 improved sub-grid representation.

1017

1018 **Code/Data Availability**

1019 The original Community Land Model is available at <https://github.com/ESCOMP/ctsm>. The source code of model
1020 development in this study is available from the corresponding author upon request.

1021 **Author contributions**

1022 L.C conducted model development work and wrote the initial draft with additional contributions from all authors.
1023 H.L, S.W, and K.S.A provided ideas and help during the process of model development. H.L provided the code
1024 of excess ice physics in the earlier version of CLM. L.C prepared all figures.

1025 **Acknowledgments**

1026 This study is funded by the Research Council of Norway KLIMAFORSK program (PERMANOR; RCN#255331).
1027 K.S.A is supported by the Research Council of Norway EMERALD project (RCN#294948). We thank Sarah
1028 Chadburn for helpful comments and suggestions in preparing this manuscript.

1029

1030 **Reference**

1031 Aas, K. S., Martin, L., Nitzbon, J., Langer, M., Boike, J., Lee, H., Berntsen, T. K., and Westermann, S.: Thaw
1032 processes in ice-rich permafrost landscapes represented with laterally coupled tiles in a land surface
1033 model, *The Cryosphere*, 13, 591-609, 10.5194/tc-13-591-2019, 2019.

1034 Brown, J., Ferrians Jr, O., Heginbottom, J., and Melnikov, E.: Circum-Arctic map of permafrost and ground-ice
1035 conditions, US Geological Survey Reston, VA, 1997.

1036 Burke, E. J., Dankers, R., Jones, C. D., and Wiltshire, A. J.: A retrospective analysis of pan Arctic permafrost using
1037 the JULES land surface model, *Climate Dynamics*, 41, 1025-1038, 10.1007/s00382-012-1648-x, 2013.

1038 Cable, S., Elberling, B., and Kroon, A.: Holocene permafrost history and cryostratigraphy in the High-Arctic
1039 Adventdalen Valley, central Svalbard, *Boreas*, 47, 423-442, 10.1111/bor.12286, 2018.

1040 Calmels, F., and Allard, M.: Segregated ice structures in various heaved permafrost landforms through CT Scan,
1041 *Earth Surface Processes and Landforms*, 33, 209-225, 10.1002/esp.1538, 2008.

1042 Collier, N., Hoffman, F. M., Lawrence, D. M., Keppel-Aleks, G., Koven, C. D., Riley, W. J., Mu, M., and
1043 Randerson, J. T.: The International Land Model Benchmarking (ILAMB) system: design, theory, and
1044 implementation, *Journal of Advances in Modeling Earth Systems*, 10, 2731-2754, 2018.

1045 Ekici, A., Lee, H., Lawrence, D. M., Swenson, S. C., and Prigent, C.: Ground subsidence effects on simulating
1046 dynamic high-latitude surface inundation under permafrost thaw using CLM5, *Geosci. Model Dev.*, 12,
1047 5291-5300, 10.5194/gmd-12-5291-2019, 2019.

1048 Fedorova, I., Chetverova, A., Bolshiyarov, D., Makarov, A., Boike, J., Heim, B., Morgenstern, A., Overduin, P.

1049 P., Wegner, C., Kashina, V., Eulenburg, A., Dobrotina, E., and Sidorina, I.: Lena Delta hydrology and
1050 geochemistry: long-term hydrological data and recent field observations, *Biogeosciences*, 12, 345-363,
1051 10.5194/bg-12-345-2015, 2015.

1052 Fisher, R. A., and Koven, C. D.: Perspectives on the future of Land Surface Models and the challenges of
1053 representing complex terrestrial systems, *Journal of Advances in Modeling Earth Systems*, n/a,
1054 10.1029/2018MS001453, 2020.

1055 Fritz, M., Wetterich, S., Meyer, H., Schirmer, L., Lantuit, H., and Pollard, W. H.: Origin and characteristics
1056 of massive ground ice on Herschel Island (western Canadian Arctic) as revealed by stable water isotope
1057 and Hydrochemical signatures, *Permafrost and Periglacial Processes*, 22, 26-38, 10.1002/ppp.714, 2011.

1058 Gilbert, G. L., Kanevskiy, M., and Murton, J. B.: Recent Advances (2008–2015) in the Study of Ground Ice and
1059 Cryostratigraphy, *Permafrost and Periglacial Processes*, 27, 377-389, 10.1002/ppp.1912, 2016.

1060 Grosse, G., Romanovsky, V., Jorgenson, T., Anthony, K. W., Brown, J., and Overduin, P. P.: Vulnerability and
1061 feedbacks of permafrost to climate change, *Eos, Transactions American Geophysical Union*, 92, 73-74,
1062 2011.

1063 Grosse, G., Robinson, J. E., Bryant, R., Taylor, M. D., Harper, W., DeMasi, A., Kyker-Snowman, E., Veremeeva,
1064 A., Schirmer, L., and Harden, J.: Distribution of late Pleistocene ice-rich syngenetic permafrost of
1065 the Yedoma Suite in east and central Siberia, Russia, US Geological Survey Open File Report, 2013, 1-
1066 37, 2013.

1067 Günther, F., Overduin, P. P., Yakshina, I. A., Opel, T., Baranskaya, A. V., and Grigoriev, M. N.: Observing
1068 Muostakh disappear: permafrost thaw subsidence and erosion of a ground-ice-rich island in response to
1069 arctic summer warming and sea ice reduction, *The Cryosphere*, 9, 151-178, 10.5194/tc-9-151-2015, 2015.

1070 [Heginbottom, J.A., Dubreuil, M.A. and Harker, P.A.: Canada, Permafrost. National Atlas of Canada. Natural](#)
1071 [Resources Canada, 5th Edition, MCR, 4177, 1995.](#)

1072 Hugelius, G., Strauss, J., Zubrzycki, S., Harden, J. W., Schuur, E. A. G., Ping, C. L., Schirmer, L., Grosse, G.,
1073 Michaelson, G. J., Koven, C. D., O'Donnell, J. A., Elberling, B., Mishra, U., Camill, P., Yu, Z., Palmtag,
1074 J., and Kuhry, P.: Estimated stocks of circumpolar permafrost carbon with quantified uncertainty ranges
1075 and identified data gaps, *Biogeosciences*, 11, 6573-6593, 10.5194/bg-11-6573-2014, 2014.

1076 Kanevskiy, M., Shur, Y., Fortier, D., Jorgenson, M. T., and Stephani, E.: Cryostratigraphy of late Pleistocene
1077 syngenetic permafrost (yedoma) in northern Alaska, Ikillik River exposure, *Quaternary Research*, 75,
1078 584-596, 10.1016/j.yqres.2010.12.003, 2011.

1079 [Iwahana, G., Fukui, K., Mikhailov, N., Ostanin, O., and Fujii, Y.: Internal Structure of a Lithalsa in the Akkol](#)
1080 [Valley, Russian Altai Mountains, 23, 107-118, 10.1002/pp](#)

1081 [Jorgenson, M., Yoshikawa, K., Kanevskiy, M., Shur, Y., Romanovsky, V., Marchenko, S., Grosse, G., Brown, J.,](#)
1082 [and Jones, B.: Permafrost characteristics of Alaska, Proceedings of the Ninth International Conference](#)
1083 [on Permafrost, 2008, 121-122.p.1734, 2012.](#)

1084 [Kanevskiy, M., Jorgenson, T., Shur, Y., O'Donnell, J. A., Harden, J. W., Zhuang, Q., and Fortier, D.:](#)

1085 [Cryostratigraphy and Permafrost Evolution in the Lacustrine Lowlands of West-Central Alaska,](#)
1086 [Permafrost and Periglacial Processes, 25, 14-34, 10.1002/ppp.1800, 2014.](#)

1087 Kim, H., Yoshimura, K., Chang, E., Famiglietti, J., and Oki, T.: Century long observation constrained global
1088 dynamic downscaling and hydrologic implication, AGU Fall Meeting Abstracts, 2012.

1089 Kokelj, S. V., Lacelle, D., Lantz, T. C., Tunnicliffe, J., Malone, L., Clark, I. D., and Chin, K. S.: Thawing of
1090 massive ground ice in mega slumps drives increases in stream sediment and solute flux across a range of
1091 watershed scales, *Journal of Geophysical Research: Earth Surface*, 118, 681-692, 10.1002/jgrf.20063,
1092 2013.

1093 Koven, C. D., Ringeval, B., Friedlingstein, P., Ciais, P., Cadule, P., Khvorostyanov, D., Krinner, G., and Tarnocai,
1094 C.: Permafrost carbon-climate feedbacks accelerate global warming, *Proceedings of the National*
1095 *Academy of Sciences*, 108, 14769-14774, 2011.

1096 Langer, M., Westermann, S., Boike, J., Kirillin, G., Grosse, G., Peng, S., and Krinner, G.: Rapid degradation of
1097 permafrost underneath waterbodies in tundra landscapes—toward a representation of thermokarst in land
1098 surface models, *Journal of Geophysical Research: Earth Surface*, 121, 2446-2470, 2016.

1099 Langer, M., Westermann, S., Heikenfeld, M., Dorn, W., and Boike, J.: Satellite-based modeling of permafrost
1100 temperatures in a tundra lowland landscape, *Remote Sensing of Environment*, 135, 12-24,
1101 <https://doi.org/10.1016/j.rse.2013.03.011>, 2013.

1102 Lawrence, D. M., Slater, A. G., Romanovsky, V. E., and Nicolsky, D. J.: Sensitivity of a model projection of near-
1103 surface permafrost degradation to soil column depth and representation of soil organic matter, *Journal of*
1104 *Geophysical Research: Earth Surface*, 113, 10.1029/2007JF000883, 2008.

1105 Lawrence, D. M., Oleson, K. W., Flanner, M. G., Thornton, P. E., Swenson, S. C., Lawrence, P. J., Zeng, X., Yang,
1106 Z. L., Levis, S., and Sakaguchi, K.: Parameterization improvements and functional and structural
1107 advances in version 4 of the Community Land Model, *Journal of Advances in Modeling Earth Systems*,
1108 3, 2011.

1109 Lawrence, D. M., Slater, A. G., and Swenson, S. C.: Simulation of present-day and future permafrost and
1110 seasonally frozen ground conditions in CCSM4, *Journal of Climate*, 25, 2207-2225, 2012.

1111 Lawrence, D. M., Koven, C. D., Swenson, S. C., Riley, W. J., and Slater, A. G.: Permafrost thaw and resulting soil
1112 moisture changes regulate projected high-latitude CO₂ and CH₄ emissions, *Environmental Research*
1113 *Letters*, 10, 094011, 10.1088/1748-9326/10/9/094011, 2015.

1114 Lawrence, D. M., Fisher, R. A., Koven, C. D., Oleson, K. W., Swenson, S. C., Bonan, G., Collier, N., Ghimire, B.,
1115 van Kampenhou, L., Kennedy, D., Kluzek, E., Lawrence, P. J., Li, F., Li, H., Lombardozi, D., Riley, W.
1116 J., Sacks, W. J., Shi, M., Vertenstein, M., Wieder, W. R., Xu, C., Ali, A. A., Badger, A. M., Bisht, G., van
1117 den Broeke, M., Brunke, M. A., Burns, S. P., Buzan, J., Clark, M., Craig, A., Dahlin, K., Drewniak, B.,
1118 Fisher, J. B., Flanner, M., Fox, A. M., Gentine, P., Hoffman, F., Keppel-Aleks, G., Knox, R., Kumar, S.,
1119 Lenaerts, J., Leung, L. R., Lipscomb, W. H., Lu, Y., Pandey, A., Pelletier, J. D., Perket, J., Randerson, J.
1120 T., Ricciuto, D. M., Sanderson, B. M., Slater, A., Subin, Z. M., Tang, J., Thomas, R. Q., Val Martin, M.,
1121 and Zeng, X.: The Community Land Model Version 5: Description of New Features, Benchmarking, and

- 1122 Impact of Forcing Uncertainty, 11, 4245-4287, 10.1029/2018ms001583, 2019.
- 1123 Lee, H., Swenson, S. C., Slater, A. G., and Lawrence, D. M.: Effects of excess ground ice on projections of
1124 permafrost in a warming climate, *Environmental Research Letters*, 9, 124006, 2014.
- 1125 Liu, L., Zhang, T., and Wahr, J.: InSAR measurements of surface deformation over permafrost on the North Slope
1126 of Alaska, *Journal of Geophysical Research: Earth Surface*, 115, 10.1029/2009jf001547, 2010.
- 1127 Loranty, M. M., and Goetz, S. J.: Shrub expansion and climate feedbacks in Arctic tundra, *Environmental
1128 Research Letters*, 7, 011005, 10.1088/1748-9326/7/1/011005, 2012.
- 1129 Nitzbon, J., Langer, M., Westermann, S., Martin, L., Aas, K. S., and Boike, J.: Pathways of ice-wedge degradation
1130 in polygonal tundra under different hydrological conditions, *The Cryosphere*, 13, 1089-1123, 10.5194/tc-
1131 13-1089-2019, 2019.
- 1132 Nitzbon, J., Westermann, S., Langer, M., Martin, L. C. P., Strauss, J., Laboor, S., and Boike, J.: Fast response of
1133 cold ice-rich permafrost in northeast Siberia to a warming climate, *Nature Communications*, 11, 2201,
1134 10.1038/s41467-020-15725-8, 2020.
- 1135 O'Neill, H. B., Wolfe, S. A., and Duchesne, C.: New ground ice maps for Canada using a paleogeographic
1136 modelling approach, *The Cryosphere*, 13, 753-773, 10.5194/tc-13-753-2019, 2019.
- 1137 Pascale, G. P. D., Pollard, W. H., and Williams, K. K. J. J. o. G. R. A.: Geophysical mapping of ground ice using
1138 a combination of capacitive coupled resistivity and ground-penetrating radar, *Northwest Territories,
1139 Canada*, 113, 2008.
- 1140 Rachold, V., and Grigoriev, M.: Russian-German Cooperation SYSTEM LAPTEV SEA 2000: The Lena Delta
1141 1998 Expedition, *Berichte zur Polarforschung (Reports on Polar Research)*, 315, 1999.
- 1142 Schaefer, K., Lantuit, H., Romanovsky, V. E., Schuur, E. A. G., and Witt, R.: The impact of the permafrost carbon
1143 feedback on global climate, *Environmental Research Letters*, 9, 085003, 10.1088/1748-9326/9/8/085003,
1144 2014.
- 1145 Schirrmeister, L., Grosse, G., Schwamborn, G., Andreev, A. A., Meyer, H., Kunitsky, V. V., Kuznetsova, T. V.,
1146 Dorozhkina, M. V., Pavlova, E. Y., Bobrov, A. A., and Oezen, D.: Late Quaternary History of the
1147 Accumulation Plain North of the Chekanovsky Ridge (Lena Delta, Russia): A Multidisciplinary
1148 Approach, *Polar Geography*, 27, 277-319, 10.1080/789610225, 2003.
- 1149 Schirrmeister, L., Grosse, G., Schnelle, M., Fuchs, M., Krbetschek, M., Ulrich, M., Kunitsky, V., Grigoriev, M.,
1150 Andreev, A., Kienast, F., Meyer, H., Babiy, O., Klimova, I., Bobrov, A., Wetterich, S., and Schwamborn,
1151 G.: Late Quaternary paleoenvironmental records from the western Lena Delta, Arctic Siberia,
1152 *Palaeogeography, Palaeoclimatology, Palaeoecology*, 299, 175-196,
1153 <https://doi.org/10.1016/j.palaeo.2010.10.045>, 2011.
- 1154 Schirrmeister, L., Froese, D., Tumskey, V., Grosse, G., and Wetterich, S.: Yedoma: Late Pleistocene ice-rich
1155 syngenetic permafrost of Beringia, in: *Encyclopedia of Quaternary Science*. 2nd edition, Elsevier, 542-
1156 552, 2013.
- 1157 Schneider, J., Grosse, G., and Wagner, D.: Land cover classification of tundra environments in the Arctic Lena

1158 Delta based on Landsat 7 ETM+ data and its application for upscaling of methane emissions, Remote
1159 Sensing of Environment, 113, 380-391, <https://doi.org/10.1016/j.rse.2008.10.013>, 2009.

1160 Schuur, E. A., Bockheim, J., Canadell, J. G., Euskirchen, E., Field, C. B., Goryachkin, S. V., Hagemann, S., Kuhry,
1161 P., Lafleur, P. M., and Lee, H.: Vulnerability of permafrost carbon to climate change: Implications for the
1162 global carbon cycle, *BioScience*, 58, 701-714, 2008.

1163 Schuur, E. A. G., McGuire, A. D., Schädel, C., Grosse, G., Harden, J. W., Hayes, D. J., Hugelius, G., Koven, C.
1164 D., Kuhry, P., Lawrence, D. M., Natali, S. M., Olefeldt, D., Romanovsky, V. E., Schaefer, K., Turetsky,
1165 M. R., Treat, C. C., and Vonk, J. E.: Climate change and the permafrost carbon feedback, *Nature*, 520,
1166 171, [10.1038/nature14338](https://doi.org/10.1038/nature14338), 2015.

1167 Schwamborn, G., Rachold, V., and Grigoriev, M. N.: Late Quaternary sedimentation history of the Lena Delta,
1168 *Quaternary International*, 89, 119-134, [https://doi.org/10.1016/S1040-6182\(01\)00084-2](https://doi.org/10.1016/S1040-6182(01)00084-2), 2002.

1169 [Seppälä, M.: Synthesis of studies of palsa formation underlining the importance of local environmental and](https://doi.org/10.1016/j.yqres.2010.09.007)
1170 [physical characteristics, *Quaternary Research*, 75, 366-370, https://doi.org/10.1016/j.yqres.2010.09.007,](https://doi.org/10.1016/j.yqres.2010.09.007)
1171 [2011.](https://doi.org/10.1016/j.yqres.2010.09.007)

1172 [Sharkhuu, N.: Occurrence of frost heaving in the Selenge River Basin, Mongolia, 10, 187-192,](https://doi.org/10.1002/(sici)1099-1530(199904/06)10:2<187::Aid-ppp294>3.0.Co;2-w)
1173 [10.1002/\(sici\)1099-1530\(199904/06\)10:2<187::Aid-ppp294>3.0.Co;2-w, 1999.](https://doi.org/10.1002/(sici)1099-1530(199904/06)10:2<187::Aid-ppp294>3.0.Co;2-w)

1174 Shiklomanov, N. I., Streletskiy, D. A., Little, J. D., and Nelson, F. E.: Isotropic thaw subsidence in undisturbed
1175 permafrost landscapes, *Geophysical Research Letters*, 40, 6356-6361, [10.1002/2013gl058295](https://doi.org/10.1002/2013gl058295), 2013.

1176 Slater, A. G., and Lawrence, D. M.: Diagnosing present and future permafrost from climate models, *Journal of*
1177 *Climate*, 26, 5608-5623, 2013.

1178 Streletskiy, D. A., Shiklomanov, N. I., Little, J. D., Nelson, F. E., Brown, J., Nyland, K. E., and Klene, A. E.: Thaw
1179 Subsidence in Undisturbed Tundra Landscapes, Barrow, Alaska, 1962–2015, *Permafrost and Periglacial*
1180 *Processes*, 28, 566-572, [10.1002/ppp.1918](https://doi.org/10.1002/ppp.1918), 2017.

1181 Swenson, S. C., Clark, M., Fan, Y., Lawrence, D. M., and Perket, J.: Representing Intrahillslope Lateral Subsurface
1182 Flow in the Community Land Model, *Journal of Advances in Modeling Earth Systems*, 11, 4044-4065,
1183 [10.1029/2019MS001833](https://doi.org/10.1029/2019MS001833), 2019.

1184 Treat, C. C., Natali, S. M., Ernakovich, J., Iversen, C. M., Lupascu, M., McGuire, A. D., Norby, R. J., Roy
1185 Chowdhury, T., Richter, A., Šantrůčková, H., Schädel, C., Schuur, E. A. G., Sloan, V. L., Turetsky, M. R.,
1186 and Waldrop, M. P.: A pan-Arctic synthesis of CH₄ and CO₂ production from anoxic soil incubations,
1187 *Global Biogeochemical Cycles*, 21, 2787-2803, [10.1111/gcb.12875](https://doi.org/10.1111/gcb.12875), 2015.

1188 Turetsky, M. R., Abbott, B. W., Jones, M. C., Anthony, K. W., Olefeldt, D., Schuur, E. A., Koven, C., McGuire,
1189 A. D., Grosse, G., and Kuhry, P.: Permafrost collapse is accelerating carbon release, *Nature*, 569, 32-34,
1190 2019.

1191 Ulrich, M., Grosse, G., Chabrillat, S., and Schirmer, L.: Spectral characterization of periglacial surfaces and
1192 geomorphological units in the Arctic Lena Delta using field spectrometry and remote sensing, *Remote*
1193 *Sensing of Environment*, 113, 1220-1235, <https://doi.org/10.1016/j.rse.2009.02.009>, 2009.

1194 Walter, K. M., Zimov, S. A., Chanton, J. P., Verbyla, D., and Chapin, F. S.: Methane bubbling from Siberian thaw
1195 lakes as a positive feedback to climate warming, *Nature*, 443, 71-75, 10.1038/nature05040, 2006.

1196 West, J. J., and Plug, L. J.: Time-dependent morphology of thaw lakes and taliks in deep and shallow ground ice,
1197 *Journal of Geophysical Research: Earth Surface*, 113, 10.1029/2006jf000696, 2008.

1198 Westermann, S., Langer, M., Boike, J., Heikenfeld, M., Peter, M., Etzelmüller, B., and Krinner, G.: Simulating the
1199 thermal regime and thaw processes of ice-rich permafrost ground with the land-surface model CryoGrid
1200 3, *Geosci. Model Dev.*, 9, 523-546, 10.5194/gmd-9-523-2016, 2016.

1201 [Wünnemann, B., Reinhardt, C., Kotlia, B. S., and Riedel, F.: Observations on the relationship between lake
1202 formation, permafrost activity and lithalsal development during the last 20 000 years in the Tso Kar basin,
1203 Ladakh, India, 19, 341-358, 10.1002/ppp.631, 2008.](#)

1204 Zhang, T., Barry, R. G., Knowles, K., Heginbottom, J. A., and Brown, J.: Statistics and characteristics of
1205 permafrost and ground-ice distribution in the Northern Hemisphere, *Polar Geography*, 23, 132-154,
1206 10.1080/10889379909377670, 1999.

1207 Zhang, T., Heginbottom, J. A., Barry, R. G., and Brown, J.: Further statistics on the distribution of permafrost and
1208 ground ice in the Northern Hemisphere, *Polar Geography*, 24, 126-131, 10.1080/10889370009377692,
1209 2000.

1210 Zimov, S. A., Schuur, E. A., and Chapin, F. S.: Permafrost and the global carbon budget, *Science*, 312, 1612-1613,
1211 2006.

1212

1213 **Table 1: The excess ice initialization scenario in each of the three terraces (landunits) for the Lena River**
 1214 **delta, as well as that for the single-landunit excess ice initialization case.**
 1215

Depth (after adding ice)	Volumetric Ice content	Area weight
No excess ice terrain		
N/A	0%	24.6%
Holocene ground ice terrain		
0.9-9 m	65%	66.6%
Yedoma ice complex		
0.6-20 m	90%	8.8%
Average ice single-landunit case		
0.6-0.9 m	7.92%	100%
0.9-9 m	51.21%	100%
9-20 m	7.92%	100%

1216

1217

1218

1219 **Table 2: The tiling scheme prescribing area weights of landunits for each CAPS class. The detailed CAPS**
 1220 **classes are shown in Figure 2.**

Overall visible ground ice content for each CAPS point	Tiling scheme (area weights for each excess ice category)	Eligible CAPS types
5%	<u>80% no excess ice</u> ; 20% Low	clf; clf; slf; ilf; clr; dlr; slr; ilr
15%	<u>58% no excess ice</u> ; 20% Low; 22% Medium	cmf; dmf; smf; imf; dhr; shr; ihr
15%	<u>66% no excess ice</u> ; 20% Low; 14% High	chr
25%	<u>44% no excess ice</u> ; 20% Low; 22% Medium; 14% High	dhf; shf; ihf
25%	<u>52% no excess ice</u> ; 20% Low; 28% High	chf

1221

Note: For each class, the first letter is for the permafrost extent, the second for the excess ice content, and the third for the terrain and overburden, following Brown et al. (2002).

1222 **Table 3: List of simulations conducted for this study.**

Cases	Description
Single point cases for the Lena river delta	
Triple-landunit case	Applying the sub-grid representation of excess ice. Three natural vegetated landunit initialized.
Average ice single-landunit case	Not applying the sub-grid representation of excess ice. Only one natural vegetated landunit initialized. The grid-mean excess ice content for each soil layer in the only landunit is calculated by spatially averaging those in different landunits in the triple-landunit case.
Global simulation cases	
No ice case	Not adding any excess ground ice (the original CLM5 simulation).
Sub-grid ice case	Applying the sub-grid representation of excess ice. A tiling scheme helps to “translate” excess ice conditions in the CAPS data to fit what the CLM5 requires.
Grid-average ice case	Not applying the sub-grid representation of excess ice. The grid-mean excess ice content for each soil layer is calculated by spatially averaging those in different landunits in the sub-grid ice case.

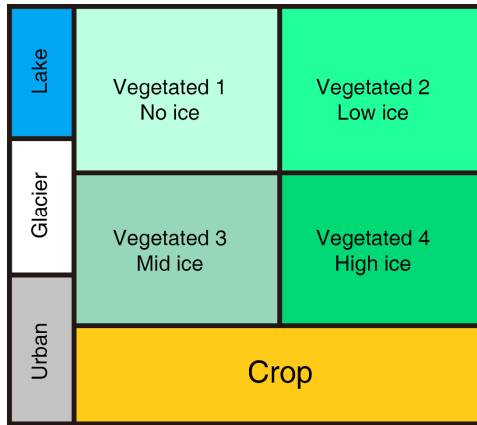
1223

1224

1225

1226

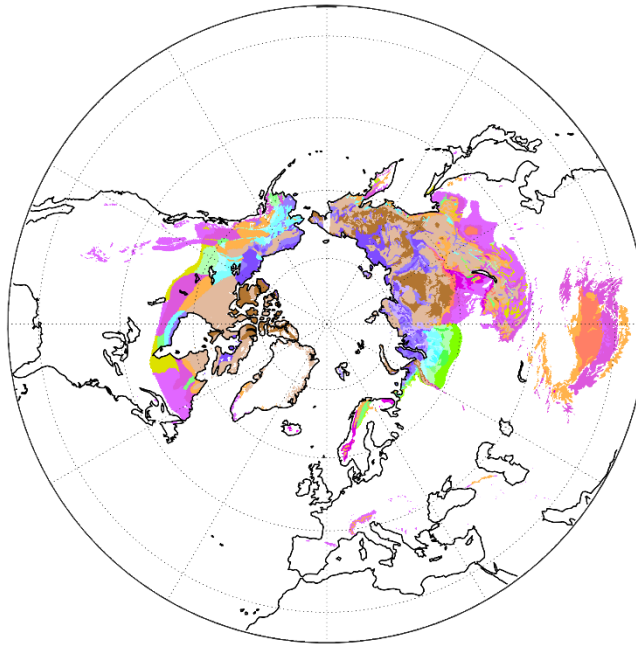
1227



1228

1229 **Figure 1: Modification of the CLM5 tiling hierarchy on the landunit level containing four natural vegetated**
 1230 **landunits for different excess ice conditions.**

1231



Permafrost area classification

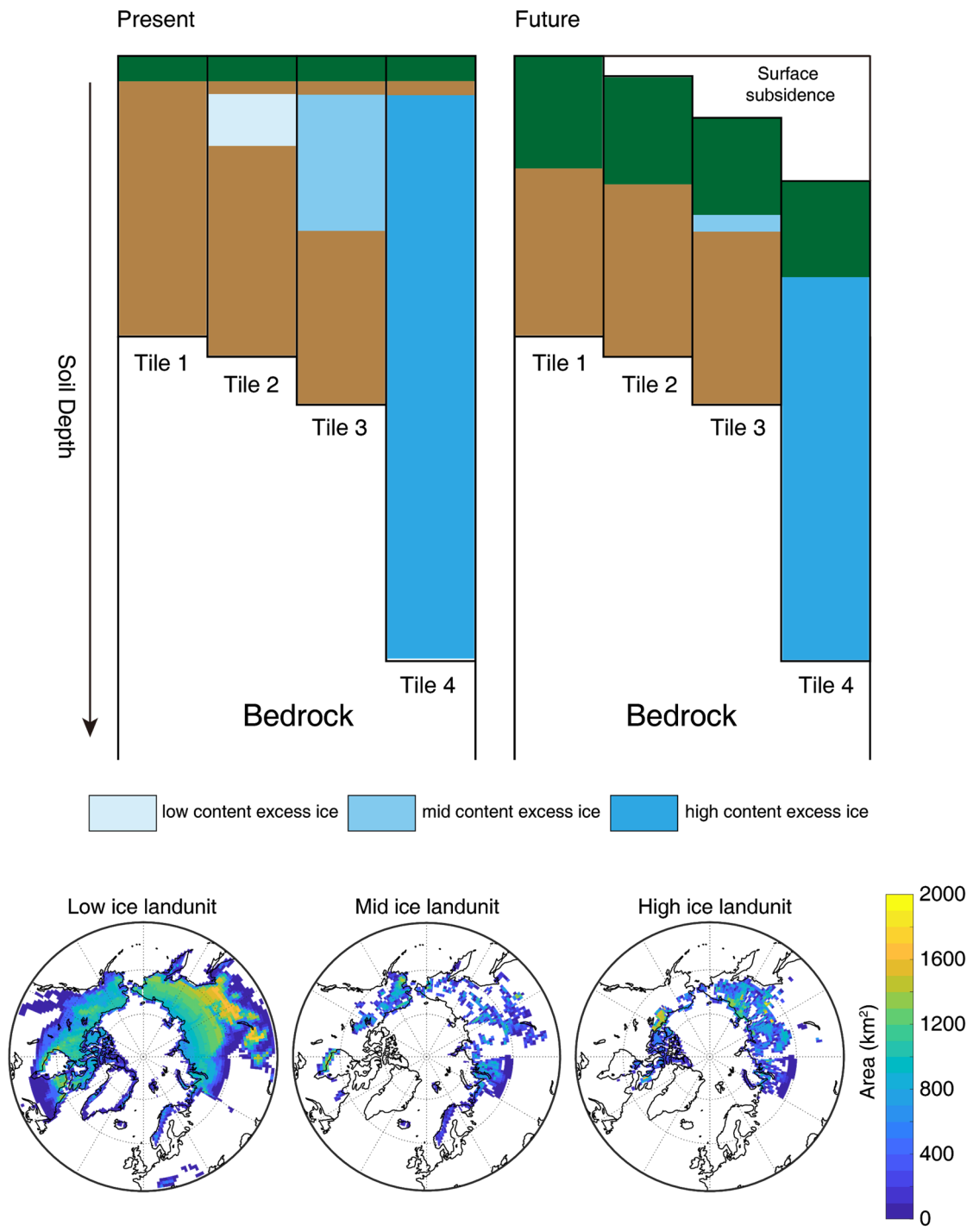
Permafrost Extent	Ground Ice Content (percent by volume)				
	Lowlands, highlands, and intra-and intermontane depressions			Mountains, highlands, ridges, and plateaus	
	25%	15%	5%	15%	5%
Continuous (100%)	chf	cmf	clf	chr	clr
Discontinuous (70%)	dhf	dmf	dlf	dhr	dhr
Sporadic (30%)	shf	smf	slf	shr	slr
Isolated (5%)	ihf	imf	ilf	ihr	ilr

* Letter code naming: The first letter is for the permafrost extent, second for the ground excess ice concent, and the thrid for the terrain and overburden.

1232

1233 **Figure 2: Spatial distribution of excess ground ice in the Northern Hemisphere modified from Brown et al.**
 1234 **(2002). Compared to the original data, permafrost extents and ground ice contents are converted to definite**
 1235 **numbers (percentages) for model computation.**

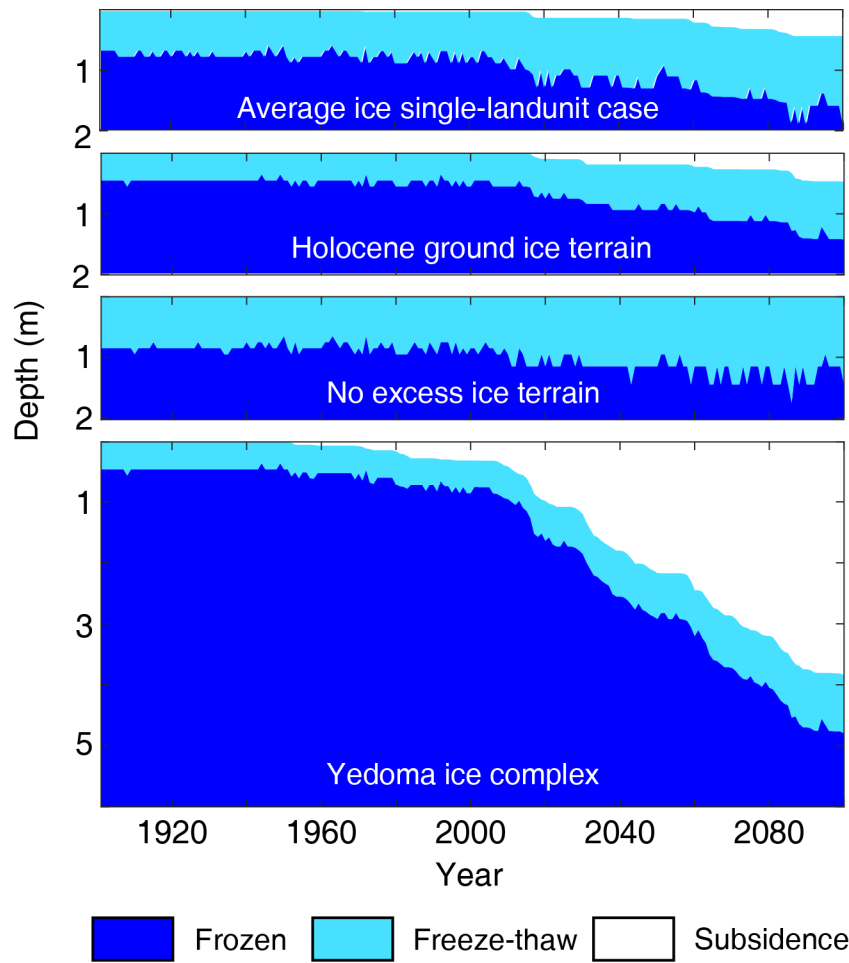
1236



1238

1239 **Figure 3. Schematic representation of the sub-grid excess ice initialization scenario, and maps showing the**
 1240 **area occupied by different excess ice landunits, i.e. the initial condition of excess ice in the global simulation.**

1241



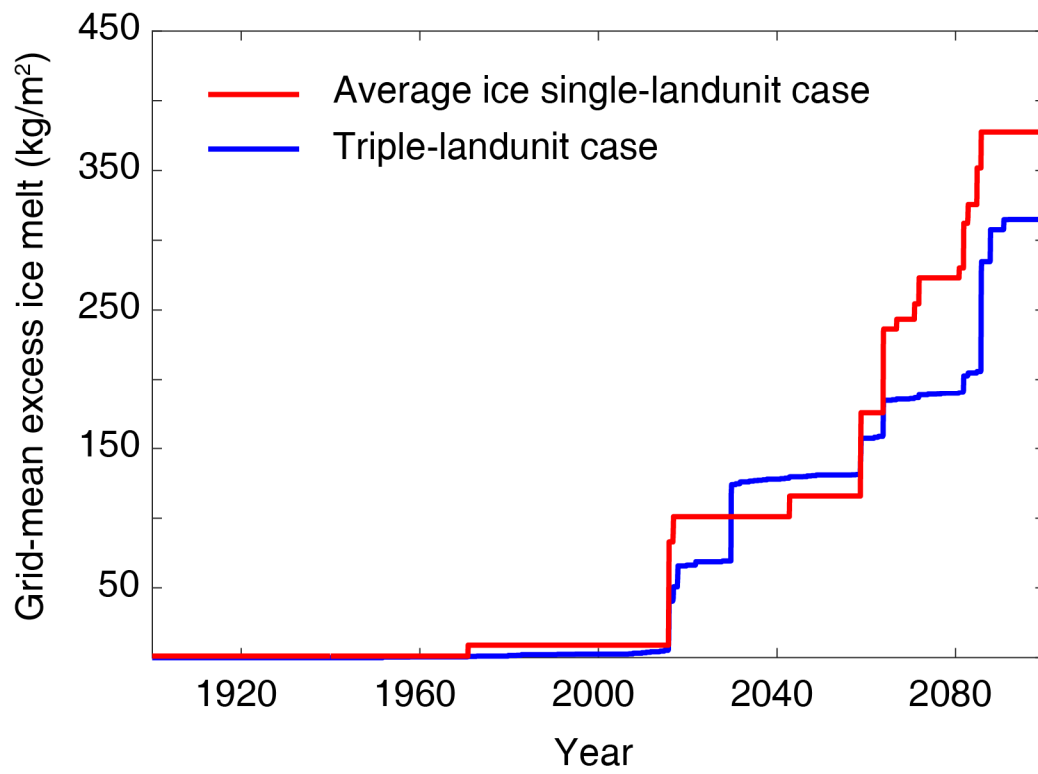
1242

1243

1244

1245

Figure 4. Annual freeze-thaw state for the three terraces for the triple-landunit case, as well as for the average ice single-landunit case.

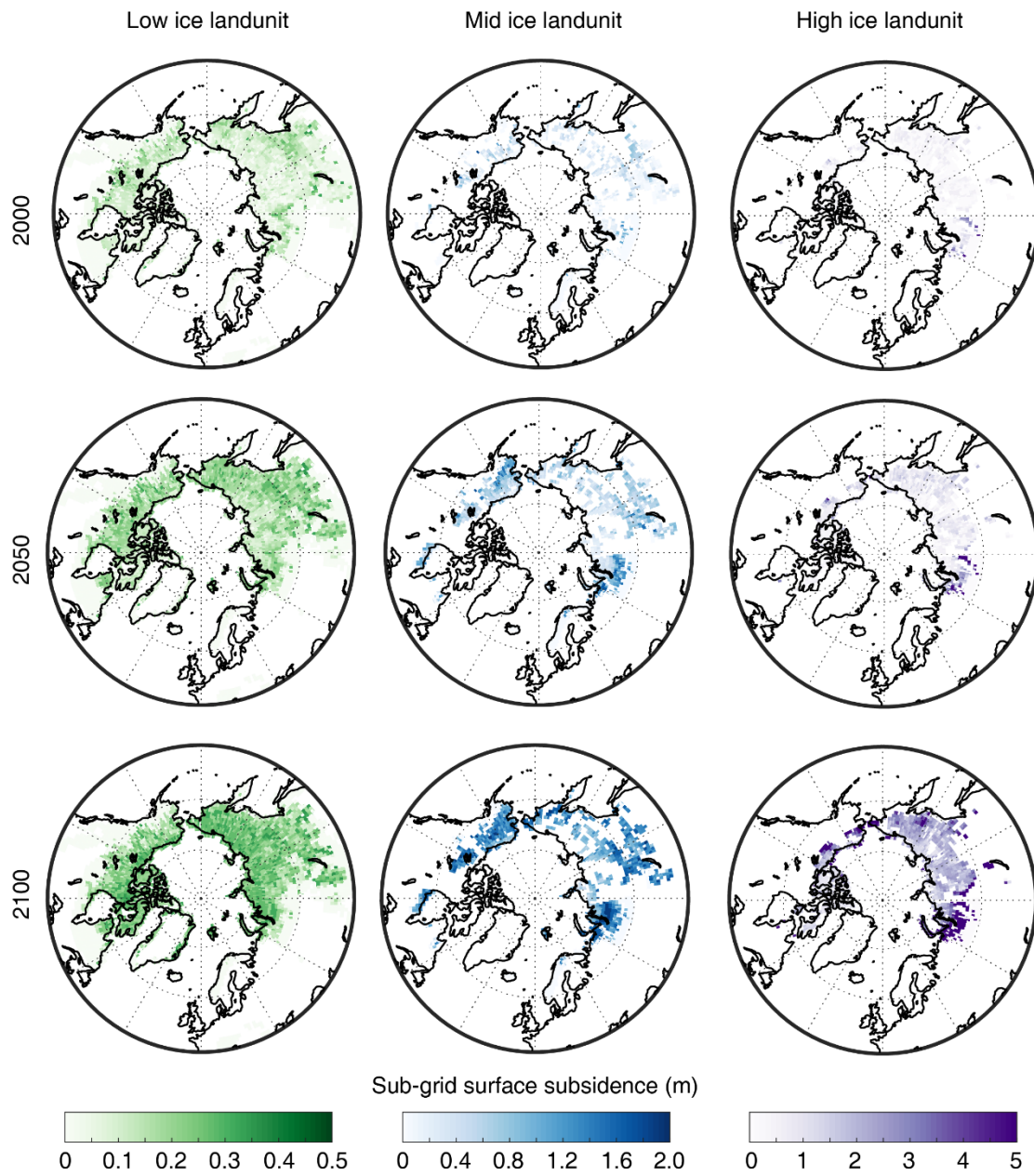


1246

1247 **Figure 5. Grid-mean excess ice melt since 1900 for the single-point cases over the Lena river delta with and**

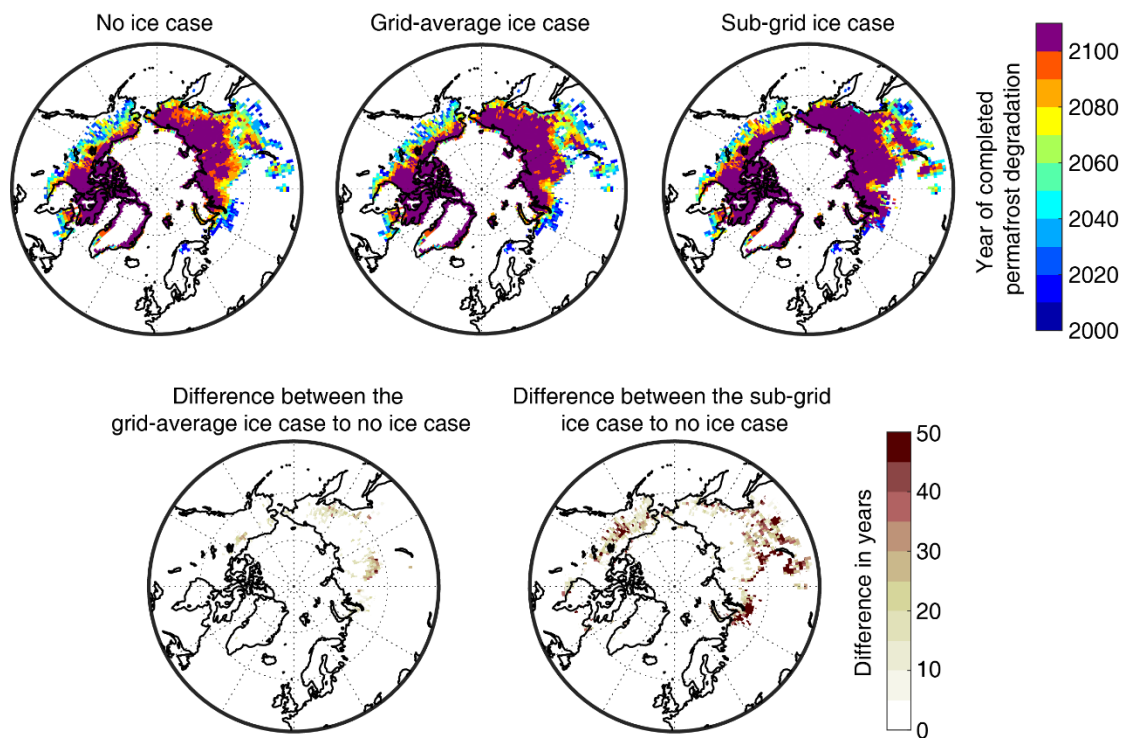
1248 **without the sub-grid excess ice initialization.**

1249



1250
1251
1252
1253

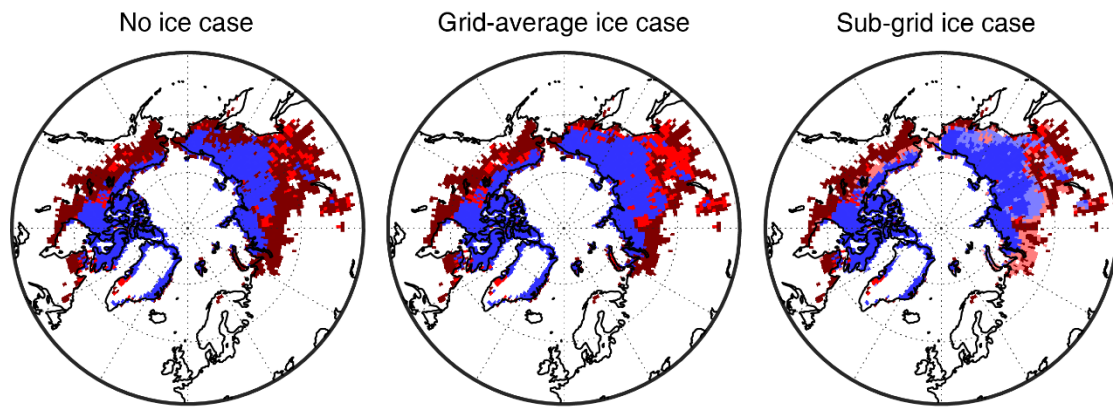
Figure 6. Maps showing sub-grid surface subsidence (m) in 2000, 2050, 2100 in the low, mid, and high excess ice landunits in the sub-grid ice case.



1254

1255 **Figure 7. Maps showing the year of completed permafrost degradation (upper set of three maps), as well as**
 1256 **the differences between cases (lower set of two maps). The purple color indicates the existence of permafrost**
 1257 **in these grid points by 2100. The difference in years is provided only for grid cell with completed permafrost**
 1258 **degradation before 2100.**

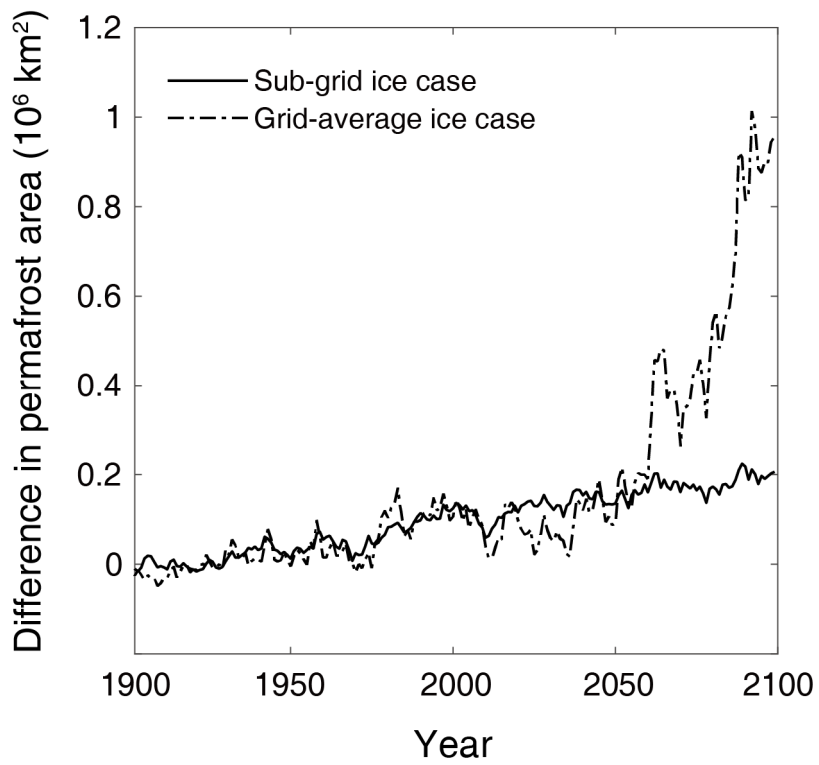
1259



■ Remaining permafrost
 ■ Partially degraded permafrost, without talik
■ Partially degraded permafrost, with talik
 ■ Fully degraded permafrost, without year-round unfrozen soil
■ Fully degraded permafrost, with year-round unfrozen soil

1260
1261
1262
1263

Figure 8. Maps of different stages of permafrost degradation diagnosed from the model output by the year 2100.



1264
1265
1266
1267
1268

Figure 9. Difference in modeled permafrost area vs. time between the sub-grid ice case and no ice case, as well as between the grid-average ice case and no ice case.